Journal of Functional Foods 107 (2023) 105641

Contents lists available at ScienceDirect

Journal of Functional Foods

journal homepage: www.elsevier.com/locate/jff

Essential oil and polyphenolics from *Thymus satureioides* Coss. counteract acrylamide-induced liver toxicity through suppression of NLRP3 inflammasome/NF-κB axis

Mona F. Mahmoud [a,*], Rania A. Elrashidy [b], Heba Osama Mohammed [c], Badreddine Drissi [d], Ismail Mahdi [d], Mansour Sobeh [d,*]

[a] Department of Pharmacology and Toxicology, Faculty of Pharmacy, Zagazig University, Zagazig 44519, Egypt
[b] Biochemistry Department, Faculty of Pharmacy, Zagazig University, Zagazig 44519, Egypt
[c] Human Anatomy and Embryology Department, Faculty of Medicine, Zagazig University, Zagazig 44519, Egypt
[d] Agrobiosciences Program, College for Sustainable Agriculture and Environmental Science, Mohammed VI Polytechnic University, Ben-Guerir 43150, Morocco

ARTICLE INFO

Keywords:
Thymus satureioides
Acrylamide
Liver toxicity
Collagen deposition
NLRP3 inflammasome/NF-κB axis

ABSTRACT

Acrylamide is a carcinogenic, mutagenic and reprotoxic substance to humans through the intense oxidative stress it induces. As the liver is the most important organ in detoxifying toxic agents, we investigated here the hepatoprotective potential of *Thymus satureioides* aerial parts extract and their essential oil, profiled by LC–MS/MS and GC–MS, respectively, on acrylamide-induced liver toxicity *in vivo*. Adult male Wistar albino rats were randomly assigned into six equal groups, namely the negative control group (10% w/v gum acacia and corn oil), the acrylamide group (10% gum acacia and corn oil + acrylamide (25 mg/kg/day)), *T. satureioides* polyphenols-treated group (100 and 200 mg/kg/day + acrylamide (25 mg/kg/day)), *T. satureioides* essential oil-treated group (EO, 0.25 ml/kg/day + acrylamide (25 mg/kg/day)), and silymarin group (Positive control) (100 mg/kg/day + acrylamide (25 mg/kg/day)). Liver toxicity was monitored by measuring liver enzyme activities, oxidative stress markers, NLRP3 inflammasome and inflammatory markers, apoptosis signaling, immunohistochemical study and morphometric analysis. Acrylamide administration substantially elevated serum liver enzymes AST, ALT, and serum total bilirubin, altered liver architecture, decreased hepatic GSH, increased hydropic cells scoring, collagen fibre deposition, immunoexpression of liver fibrotic markers (MMP9 and TGF-1β), lipid peroxidation (MDA), inflammatory responses (IL-1β and p38 MAPK) in hepatic tissues, upregulated liver NLRP3 inflammasome activation, and augmented NF-κB and caspase 3 signaling pathways. These toxicity manifestations were significantly counteracted when rats were pretreated with either *T. satureioides* polyphenolics or EO as well as silymarin, the reference hepatoprotective compound. Both the polyphenolics and EO furnished comparable mitigation effects to those obtained using silymarin. The observed hepatoprotective activities could be attributed to presence of diverse metabolites (EO (39 compounds) and the extract (45 compounds)) with pronounced antioxidant and anti-inflammatory activities. This study strongly shows the effectiveness of *T. satureioides* polyphenolics and essential oil in mitigating acrylamide-induced liver toxicity.

1. Introduction

Exposure to environmental substances on a quotidian basis is one of the most important risk factors in disease development. In the vast majority of cases, these materials provoke the organism to produce reactive oxygen species (ROS) that induce cell injury, lipid peroxidation and disruption of organ function (Elhelaly et al., 2019; Kehrer and Klotz, 2015). Liver is one of the most impacted organs by free radicals and its damage might lead to severe diseases and health issues (Seto and Mandell, 2021). Despite the critical importance of liver and the high morbidity rates related to its dysfunction, the current medications designed to hinder the progression of liver diseases are still insufficient (Hussein et al., 2020) and most of them are associated with serious side effects (Schuppan et al., 2018). This have heightened the need for holistic practices advocating safe molecules with minor adverse effects. In this regard, phytotherapy is a promising science-based practice for the

* Corresponding authors.
E-mail addresses: mona_pharmacology@yahoo.com, mfabdelaziz@zu.edu.eg (M.F. Mahmoud), mansour.sobeh@um6p.ma (M. Sobeh).

https://doi.org/10.1016/j.jff.2023.105641
Received 31 March 2023; Received in revised form 27 May 2023; Accepted 18 June 2023
Available online 24 June 2023

Table 1
Volatile constituents of *T. satureioides* aerial parts' essential oil.

No.	Name compounds	Relative abundance (%)	Retention index	
			Calculated	**Reported**
1	Tricyclene	0.1	918	921
2	α-Thujene	0.12	923	924
3	α-Pinene	1.34	931	932
4	Camphene	2.67	948	946
5	β-Pinene	0.24	981	974
6	Myrcene	0.33	988	988
7	Octan-3-ol	0.09	993	993
8	δ-2-Carene	0.02	1007	1001
9	δ-3-Carene	0.52	1015	1008
10	*O*-Cymene	3.14	1026	1022
11	D-Limonene	0.49	1034	1024
12	Eucalyptol	0.02	1035	1026
13	γ-Terpinene	1.80	1060	1054
14	*trans*-Linalool oxide	0.02	1085	1084
15	Terpinolene	0.21	1093	1086
16	Linalool	2.10	1105	1098
17	(Z)-β-Ocimene	0.03	1125	1032
18	*trans*-ρ-Menth-2-en-1-ol	0.05	1137	1136
19	neo-Menthol	0.03	1161	1161
20	Menthol	0.07	1169	1167
21	2-Methyl isoborneol	19.42	1188	1178
22	*trans*-p-Mentha-1(7),8-dien-2-ol	1.30	1191	1187
23	*trans*-Dihydro carvone	0.40	1201	1200
24	2-Octen-1-ol	12.89	1218	1208
25	Pulegone	0.15	1229	1233
26	Carvacrol, methyl ether	0.05	1238	1241
27	Anisole	5.41	1248	1241
28	Geranial	0.06	1264	1264
29	Bornyl acetate	1.23	1292	1284
30	Thymol	37.16	1297	1289
31	2-hydroxy-ρ-cymene	0.15	1300	1298
32	3-Hydroxy-p-cymene	2.16	1306	1298
33	β-caryophyllene	3.73	1422	1417
34	β-Humulene	0.40	1440	1436
35	α-Humulene	0.18	1453	1452
36	γ-Cadinene	0.10	1508	1513
37	δ-Cadinene	0.12	1523	1522
38	Caryophyllene oxide	0.59	1589	1582
39	α-Cadinol	0.34	1650	1652

prevention and treatment of such health conditions (Falzon and Balabanova, 2017; Mahdi et al., 2022). It has aroused the interest of the scientific community because of its natural feature, effectiveness, and multi-beneficial effects (Haidara et al., 2016; Posadzki et al., 2013).

Acrylamide is a crystallized monomer which dissolves easily in water and ethanol (Soliman et al., 2021). It is a highly toxic compound that forms during cooking at high temperature of meals rich in carbohydrates and proteins via asparagine-glucose reaction (Soliman et al., 2021; Tareke et al., 2002). Its polymer (polyacrylamide) is used in water treatment, textile, printing, and cosmetic sectors (Gedik et al., 2017; Jiang et al., 2021; Moorman et al., 2012). With low molecular weight and high solubility, acrylamide readily crosses the skin, respiratory and digestive systems, blood/ placenta and blood/ milk barriers (Fuhr et al., 2006; Turkington and Mitchell, 2010). Additionally, protein moieties (NH_2 and SH), nucleic acids and vinyl groups facilitate acrylamide to pass through biological membranes (Adams et al., 2010). Acrylamide is a CMR substance (carcinogenic, mutagenic and reprotoxic). It toxicity has been shown in many studies both *in vitro* and *in vivo* in animal models and humans as a promoter of testicular and thyroid cancer, as well as breast fibroadenomas (Erdemli et al., 2018; Friedman et al., 1995). Moreover, acrylamide administration has been shown to induce hepatocyte necrosis, increase hepatic enzymes, and inflammatory cell infiltration (Erdemli et al., 2018, 2017). Elsewhere, toxification by acrylamide caused both hepatic and renal injuries through oxidative stress, lipid peroxidation, DNA damage, and inflammatory responses (Abdel-Daim et al., 2020). Similarly, a previous study showed that acrylamide decreased the activities of glutathione peroxidase (GSH-PX) and superoxide dismutase (SOD) in IEC-6 cell lines (Jiang et al., 2021).

Thymus satureioides Coss. is one of *Thymus* species belonging to the Lamiaceae family (el-Fassi Fihri, 1998; Kabbaoui et al., 2016). It is a perennial shrub, endemic to semiarid zones of the Moroccan High Atlas and Anti-Atlas where it is vernacularly known as "Zaitra" or "Azkuni" (Bellakhdar et al., 1991; Benabid, 2000). Traditionally, this plant is used to treat many diseases such as diabetes, fever, hypertension, dermatological and circulatory disorders, bronchitis, nociception, immune system problems, pharyngitis, and influenza (El Hachlafi et al., 2021). Moreover, several pharmacological studies have demonstrated that *T. satureioides* extracts and essential oils elicit diverse biological activities such as antidiabetic (Kabbaoui et al., 2016), anticancer (Jaafari et al., 2007), anti-inflammatory (Khouya et al., 2015), antimicrobial (Amrouche et al., 2018; Asdadi et al., 2014; El Hattabi et al., 2016), insecticidal (Avato et al., 2017; Santana et al., 2014), and hypolipidemic (Ramchoun et al., 2012) properties. However, the underpinning mechanisms underlying most of these pharmacological effects have been poorly investigated (El Hachlafi et al., 2021).

To the best of our knowledge, there is no study that has so far investigated the potential hepatoprotective effect of *T. satureioides* and its mechanisms of action against acrylamide-induced liver toxicity. Therefore, we examined here the *in vivo* protective effect of the essential oil and polyphenolics from *T. satureioides* aerial parts against hepatotoxicity of acrylamide and investigated the involved pathways.

2. Material and methods

2.1. Plant material and extract preparation

Flowering aerial parts of *Thymus satureioides* Coss. were purchased from a local herbalist in Ben Guerir, Morocco. The dried plant material was subjected to hydro-distillation (150 g/L, w/v) for the isolation of essential oil (EO) and residual water extract using a Clevenger apparatus. The extraction was performed until no more EO was obtained. The residual water resulting from the hydro-distillation process was collected, filtered, concentrated using a rotary evaporator and lyophilized to get the crude extract. Collected EO and residual water extract were transferred into amber glass bottles and stored until analysis (Mahdi et al. 2023).

2.2. GC–MS analysis

GCMS-TQ8040 SHIMADZU, JAPAN was utilized. Rtx®-5MS fused-bond column (30 m length, 0.25 mm internal diameter, and 0.25 μm film thickness, Restek, PA, USA) was installed. The starting temperature was 50 °C to 300 °C with a ramp of 5 °C/min and an isotherm at 300 °C for 3 min. The injector temperature was 250 °C and helium with a flow rate of 1.5 ml/min was used as carrier gas. The conditions for the mass spectra were as follows: Ion source temp 200 °C, Interface temp: 280 °C, Mass range: 50–500 *m/z*. The samples were injected in split mode. The analysis of compounds was identified with the database NIST 2017, and the retention indices were determined via n-alkanes standards.

2.3. Animals and experimental design

Adult male Wistar albino rats weighing 140 ± 20 g were supplied from the animal facility of Faculty of Veterinary Medicine, Zagazig University, Zagazig, Egypt. They were housed in polypropylene cages and kept under standard environmental conditions including temperature (23 ± 2 °C), 12 h light/dark cycle and humidity (60 ± 10 %). Rats had free access to water and were fed on a normal chow diet. After one week acclimatization, rats were randomly assigned into six groups (n = 7) as follow:

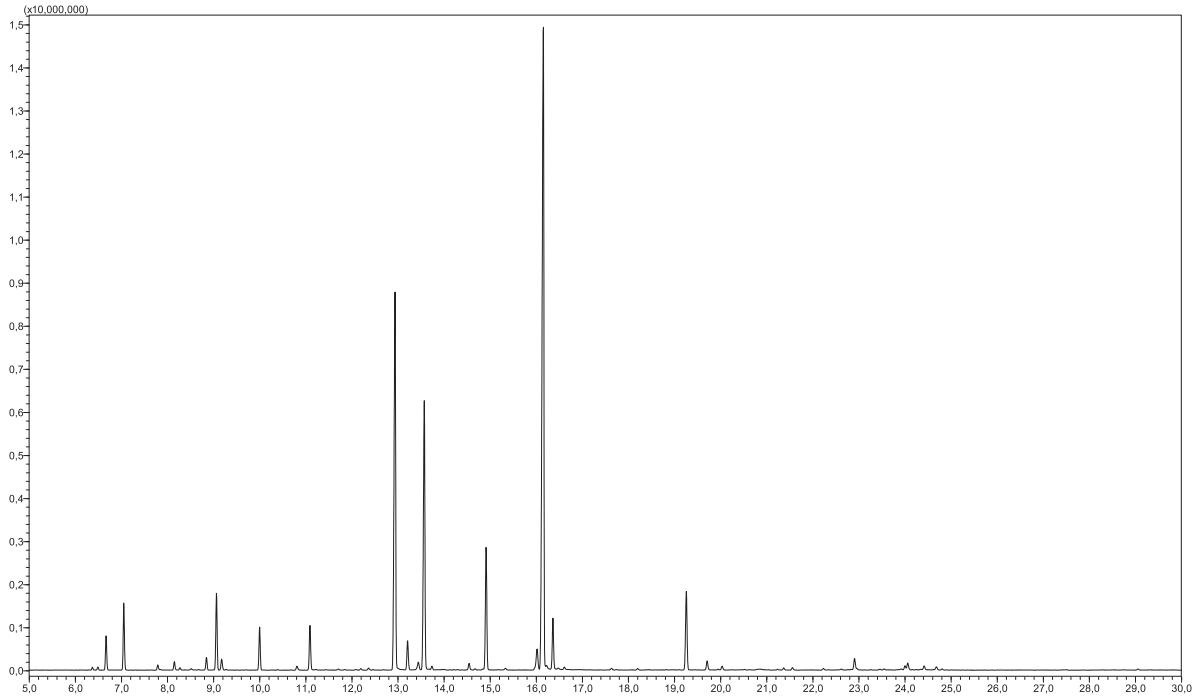

Fig. 1. GC–MS profile of the volatile constituents of *T. satureioides* aerial parts' essential oil.

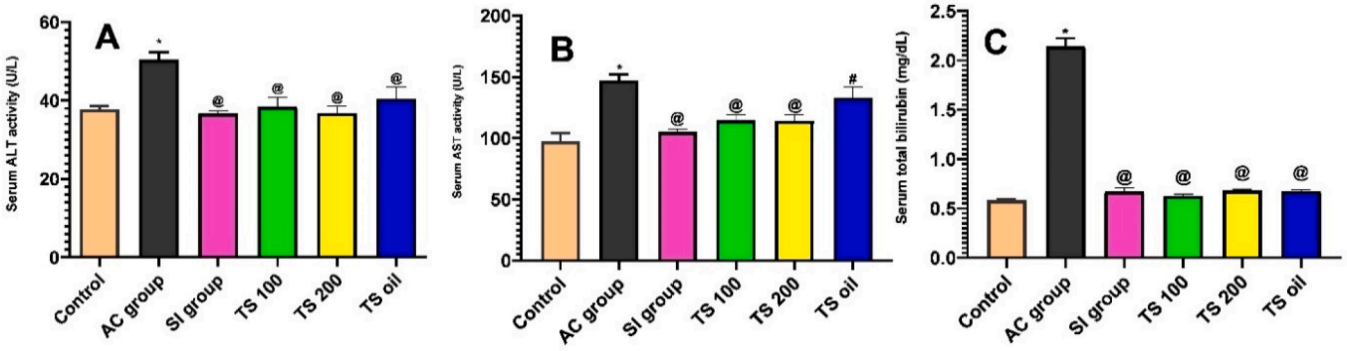

Fig. 2. Effect of acrylamide (AC, 25 mg/kg, orally), *T. satureioides* extract (TS 100 mg/kg and 200 mg/kg, orally), *T. satureioides* essential oil (TS, 0.25 ml/kg, orally) and silymarin (SI, 100 mg/kg, orally) on serum activities of AST (**A**), ALT (**B**) and serum total bilirubin level (**C**) in rats. Bars with error bars denote mean ± SE (n = 6). $^{*,@,\#}p < 0.05$ with respect to untreated control group, acrylamide-treated group and silymarin-treated group, respectively.

- Group 1 (control): Rats were treated with equal amounts of drug vehicles (10 % w/v gum acacia and corn oil) given by oral gavage for 10 consecutive days and served as control group.
- Group 2 (AC): Rats were orally pretreated with drug vehicle (10 % gum acacia and corn oil) for 3 days prior and concurrently with acrylamide (25 mg/kg/day, dissolved in distilled water) for 7 consecutive days.
- Groups 3 & 4 (TS 100 and TS 200): Rats were orally pretreated with *T. satureioides* extract (100 and 200 mg/kg/day suspended in distilled water using 10 % w/v gum acacia) and given by oral gavage for 3 days prior and concurrently with acrylamide for 7 consecutive days.
- Group 5 (TS oil): Rats were orally pretreated with *T. satureioides* essential oil (0.25 ml/kg/day dissolved in corn oil) given by oral gavage for 3 days prior and concurrently with acrylamide for 7 consecutive days.
- Group 6 (SI): Rats were orally pretreated with silymarin as a standard reference drug (100 mg/kg/day suspended in distilled water using 10 % w/v gum acacia) given by oral gavage for 3 days prior and concurrently with acrylamide for 7 consecutive days.

2.4. Blood and tissue sampling

Twenty-four hours after the last treatment, blood samples were withdrawn from the *retro*-orbital plexus under anesthesia (thiopental sodium, 40 mg/kg) and processed for serum separation. Serum aliquots were used to determine activities of liver enzymes and total bilirubin levels. Thereafter, rats were sacrificed by cervical dislocation, then livers were excised and washed in ice-cooled normal saline. Each liver is dissected into two parts. The first part was snap frozen in liquid nitrogen and stored at −80 °C for further biochemical analysis. The other part was fixed in 10% buffered formalin for 24 h for histological analysis.

2.5. Measurement of liver function markers

Serum activities of liver enzymes, AST (CAT no GOT 1121100) and ALT (CAT no GPT 115050) were determined utilizing commercially

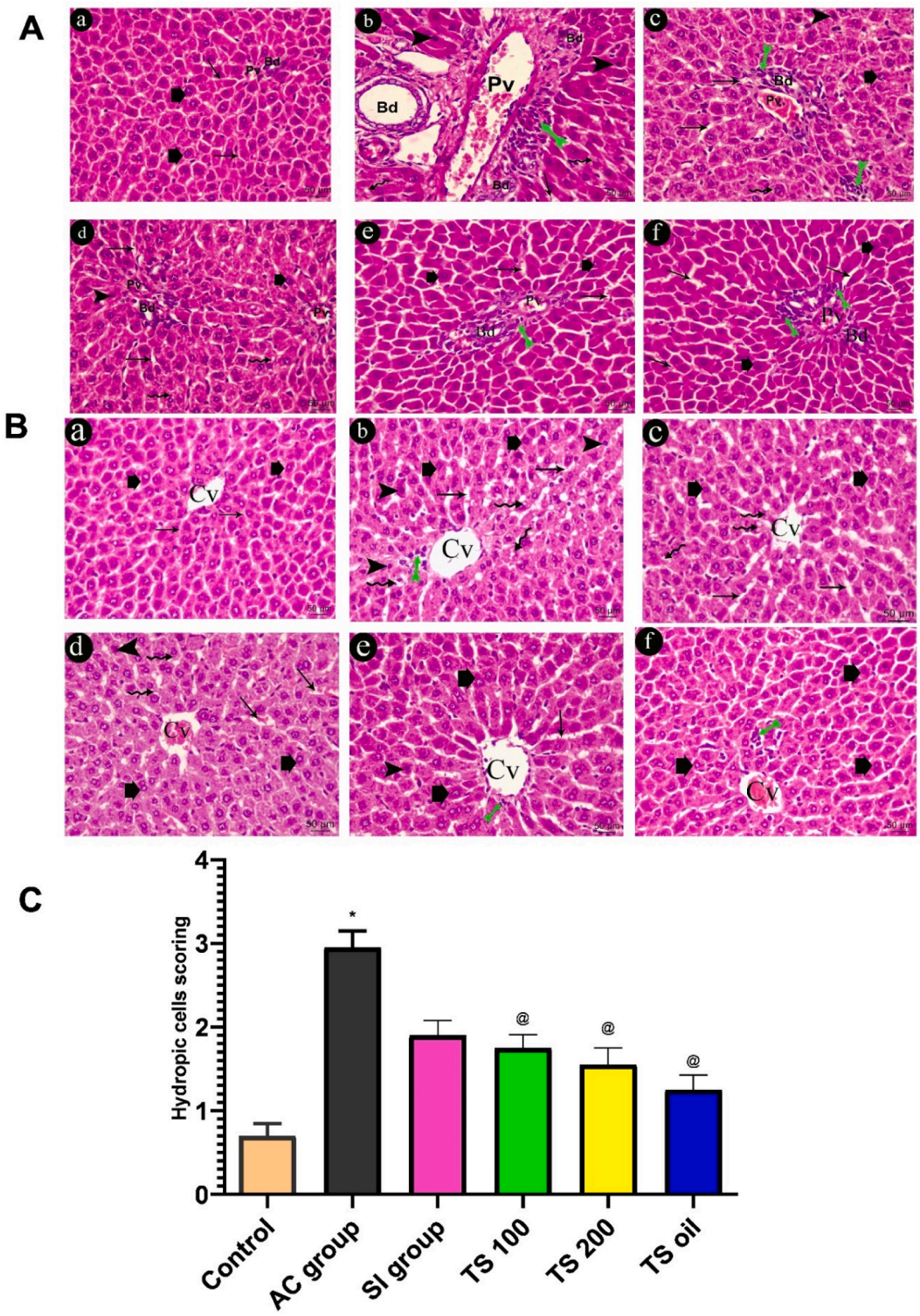

Fig. 3. Representative photomicrograph of portal area (**A**) and central vein area (**B**) of liver section in different groups. (a) control group, (b) Acrylamide group (AC, 25 mg/kg), (c) Silymarin group (SI, 100 mg/kg), (d) *T. satureioides* extract group (TS 100 mg/kg), (e) *T. satureioides* extract group (200 mg/kg), (f) *T. satureioides* essential oil group (TS oil, 0.25 ml/kg). Portal vein (Pv), central vein (Cv), bile duct (Bd), acidophilic hepatocytes with vesicular nuclei (thick arrow), sinusoids (thin arrow), vacuolated hepatocytes (zigzag arrow), dark nuclei (arrowhead), inflammatory cells (green tailed arrow), H&E 400x. **(C)** Bar chart showing statistical assessment of the histological scoring of hydropic changes area percent in different studied groups. Data are presented as mean ± SE, (five fields for each rat, n = 4 rats/group), $^{*,@}p < 0.05$ with respect to untreated control group and acrylamide-treated group, respectively using Kruskal-Wallis's test. (For interpretation of the references to colour in this figure legend, the reader is referred to the web version of this article.)

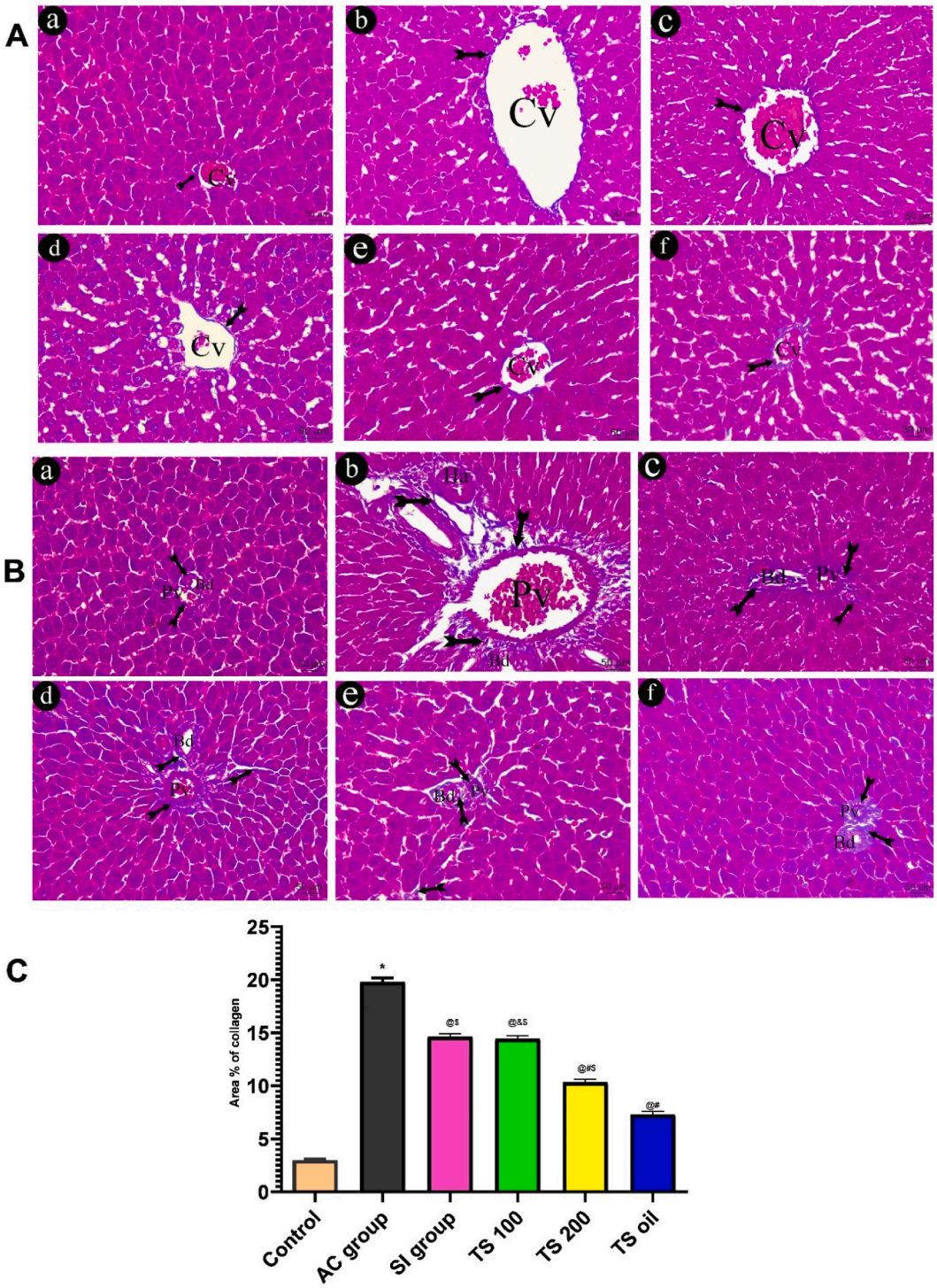

Fig. 4. A representative photomicrograph of central vein area (**A**) and portal area (**B**) of liver section stained with Mallory trichrome in different groups. (a) control group, (b) Acrylamide group (AC, 25 mg/kg), (c) Silymarin group (SI, 100 mg/kg), (d) *T. satureioides* extract group (TS 100 mg/kg), (e) *T. satureioides* extract group (200 mg/kg), (f) *T. satureioides* essential oil group (TS oil, 0.25 ml/kg). Central vein (Cv), Portal vein (Pv), Collagen fiber deposition (tailed arrow), bile duct (Bd), hepatic artery (Ha), Mallory trichrome 400x. **(C)** Bar chart showing statistical assessment of the area percentage of collagen deposits in different studied groups. The values are presented as mean ± SE (five fields for each rat, n = 4 rats/group). $^{*,@,\#,\$}p$ value < 0.05 versus control group, acrylamide group, silymarin group and essential oil group, respectively.

available kits (Biomed Diagnostic, Cairo, Egypt). Serum total bilirubin levels were determined utilizing commercially available assay kit (Diamond diagnostic, Cairo, Egypt), following the provided protocols.

2.6. Measurement of oxidative stress markers

Frozen liver tissues were homogenized in potassium phosphate (50 mM pH = 7.5), then centrifuged for 15 min at 4000rpm. The supernatant was used to measure the levels of malondialdehyde (MDA) and glutathione (GSH) using the commercially available assay kits (Biodiagnostic,

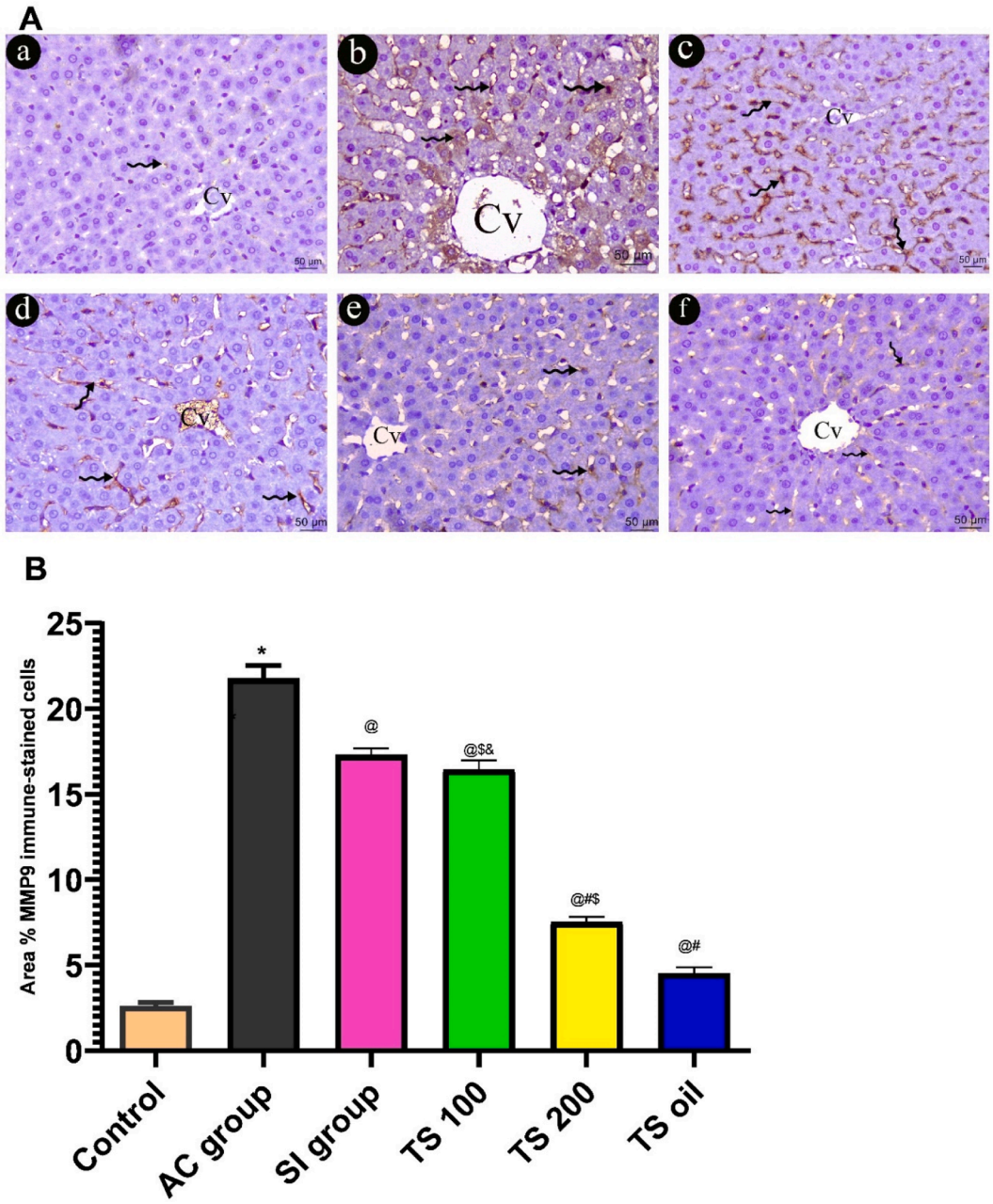

Fig. 5. (**A**) A representative photomicrograph of MMP9 immune-stained liver section in different groups. (a) control group, (b) Acrylamide group (AC, 25 mg/kg), (c) Silymarin group (SI, 100 mg/kg), (d) *T. satureioides* extract group (TS 100 mg/kg), (e) *T. satureioides* extract group (200 mg/kg), (f) *T. satureioides* essential oil group (TS oil, 0.25 ml/kg). Immune-positive cells (zigzag arrow), MMP9 immune-staining 400x. (**B**) Bar chart showing statistical assessment of the area percentage of MMP9 immune-stained cells in different studied groups using One way ANOVA test and *Tukey* HSD as a post hoc test. The values are presented as mean ± SE (five fields for each rat, n = 4 rats/group). $^{*,@,\#,\&,\$}p$ value < 0.05 versus control group, acrylamide group, silymarin group, *T. satureioides* extract group (200 mg/kg) and essential oil group, respectively.

Giza, Egypt; CAT # MD2529 and GR2511, respectively), following the manufacturers' instructions.

2.7. Measurement of NLRP3 inflammasome and inflammatory markers

Levels of NLRP3, interleukine-1beta (IL-1β), and p38 Mitogen-Activated Protein Kinase (MAPK) were measured in liver homogenates using the commercially available rat enzyme-linked immunosorbent assay (ELISA) kits (MyBioSource, San Diego, CA, USA; Catalog # MBS2033695, MBS825017 and MBS765087, respectively), according to the suppliers' protocols.

2.8. Measurement of caspase-3 activity

Caspase-3 activity was assessed in liver homogenates using the caspase-3 colorimetric assay kit (Sigma-Aldrich, Saint Louis, MI, USA; CAT #CASP-3-C). The caspase-3 activity was expressed as μmol p-nitroaniline (pNA) released per min per gram of tissue lysate.

2.9. Histological study

Specimens of liver samples were kept in 10% neutral buffered formalin and then embedded in paraffin. Serial sections of 5 μm thickness were mounted on glass slides, deparaffinized in xylene, and then

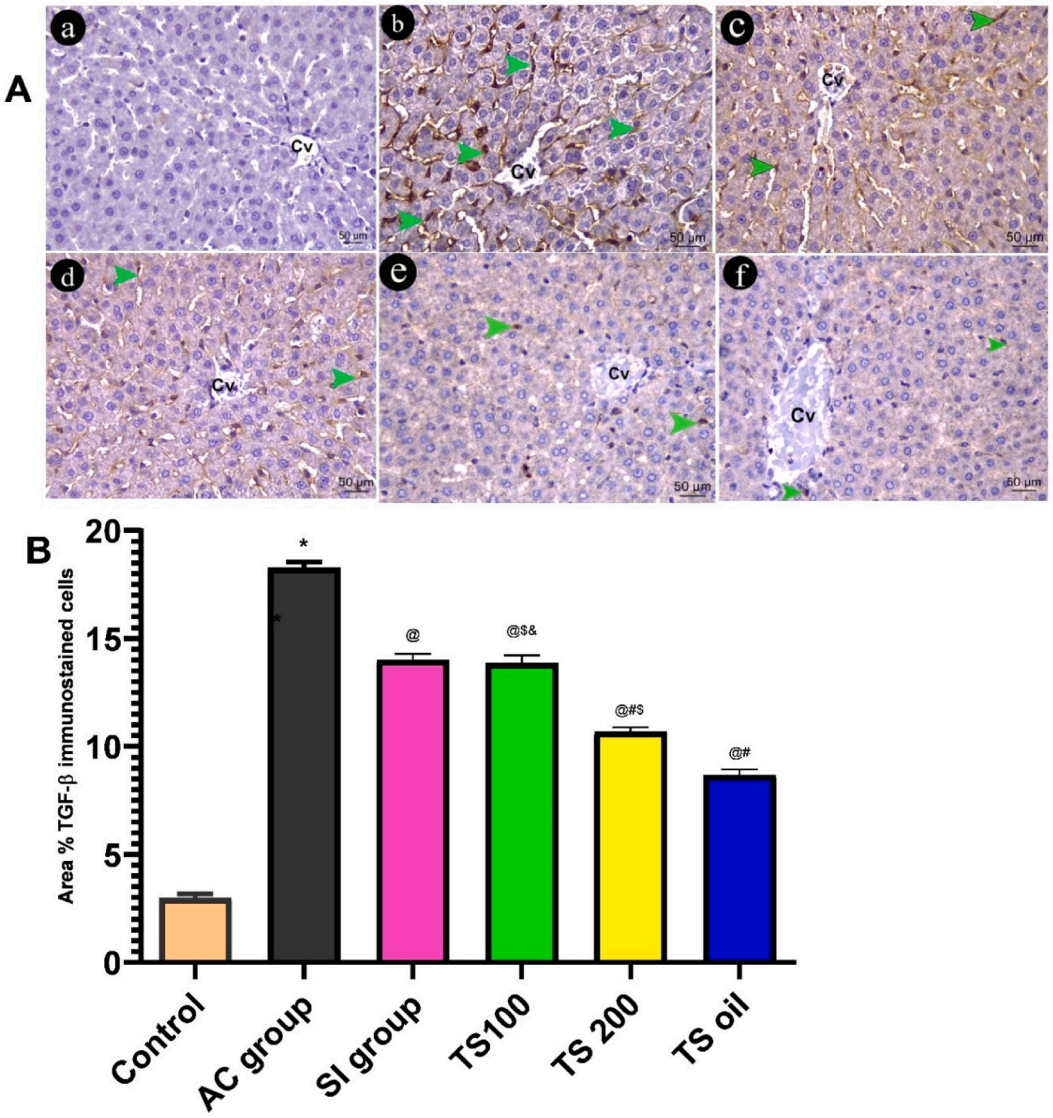

Fig. 6. (**A**) A representative photomicrograph of TGF-1β immune-stained liver section in different groups. (a) control group, (b) Acrylamide group (AC, 25 mg/kg), (c) Silymarin group (SI, 100 mg/kg), (d) *T. satureioides* extract group (TS 100 mg/kg), (e) *T. satureioides* extract group (200 mg/kg), (f) *T. satureioides* essential oil group (TS oil, 0.25 ml/kg). Central vein (Cv), immune-positive cells (green arrowhead), TGF-β immune-staining 400x. (**B**) Bar chart showing statistical assessment of the area percentage of TGF-1β immune-stained cells in different studied groups using One way ANOVA test and *Tukey* HSD as a post hoc test. The values are presented as mean ± SE (five fields for each rat, n = 4 rats/group). $^{*,@,\#,\&,\$}p$ value < 0.05 versus control group, acrylamide group, silymarin group, *T. satureioides* (200 mg/kg) extract group and essential oil group, respectively. (For interpretation of the references to colour in this figure legend, the reader is referred to the web version of this article.)

stained with Hematoxylin and eosin (H&E) and Mallory's trichrome (MT) stain according to (Bancroft, 2013). Each slide was subjected for examining by light microscopy (LeicaICC50W).

2.10. Immunohistochemical study and morphometric analysis

2.10.1. Immunostaining for NF-κβ, TNF-α, MMP9 and TGF-1β

Immunohistochemical staining was processed by applying rabbit polyclonal antibodies (NF-κB, Protein tech company, USA, catalog #10409–2-AP) used at 1/200 a concentration, TNF-α IHC antibody (polyclonal, Abbiotec, USA) at 1:80 diluted in phosphate buffered saline (PBS), the anti-matrix metalloproteinase-9 antibody (MMP-9, 1:1000, ab76003, Abcam), and rabbit polyclonal antibody for TGF-1β (Santa Cruz Biotechnology, San Francisco, CA, USA) at 4 µg/mL overnight at 4 °C. The slides were deparaffinized followed by washing in PBS. A peroxidase blocking solution (3% H_2O_2 in methanol) was used to reduce endogenous peroxidases for 15 min then washed by tris buffer saline (TBS). To block nonspecific binding of IgG, normal goat serum was used, diluted 1: 50 in 0.1 % bovine serum albumin with TBS for half an hour, primary antibodies were added on slides and left overnight at room temperature. Then, slides were subjected for washing in buffer and incubated for further 30 min with biotinylated goat anti-rabbit secondary antibodies diluted 1: 1000, followed by several washing. The slides incubated for 30 min with vectastain Avidin, Biotinylated horse radish peroxidase Complex kits and washed for 10 min, the substrate, diaminobenzidine tetra hydrochloride in distilled water was applied for 5–10 min. Slides were counter stained by hematoxylin. For negative control slides, we repeated the previous steps without addition of the primary antibody (Akahoshi et al., 2002, Ramos-Vara et al., 2008, Kim et al., 2011, Xu et al., 2017).

2.10.2. Morphometric analysis

To perform morphometrical analysis, four rats per group were tested. Five randomly selected non-overlapping fields from slides of each

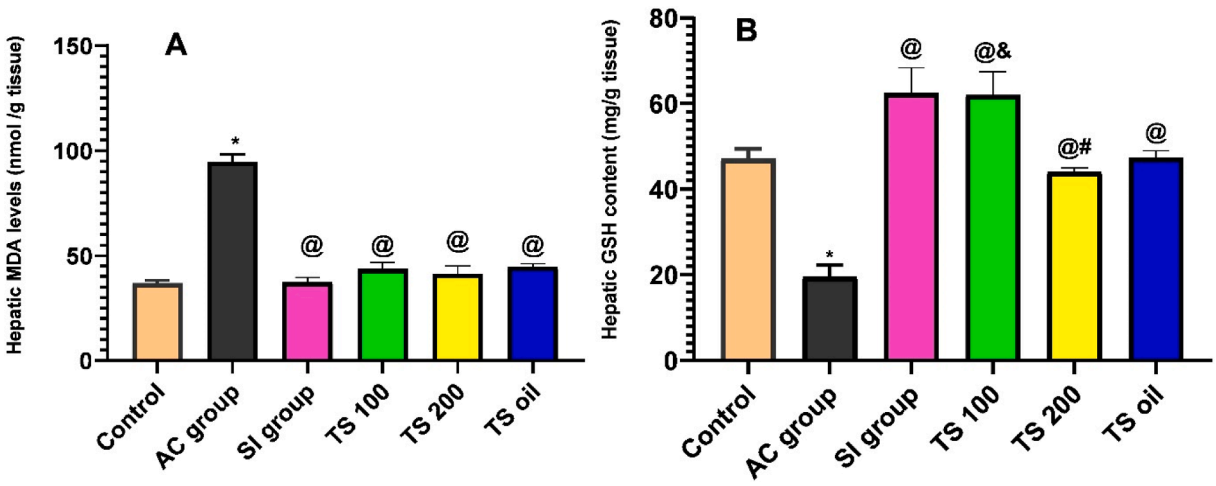

Fig. 7. Effect of acrylamide (AC, 25 mg/kg), *T. satureioides* extract (TS, 100 mg/kg and 200 mg/kg), *T. satureioides* essential oil (TS, 0.25 ml/kg) and silymarin (SI, 100 mg/kg) on hepatic levels of MDA (**A**) and GSH (**B**) in rats. Bars with error bars denote mean ± SE (n = 5–6). $^{*,@,\#,\&}p$ value < 0.05 versus control group, acrylamide group, silymarin group, and *T. satureioides* (200 mg/kg) extract group, respectively.

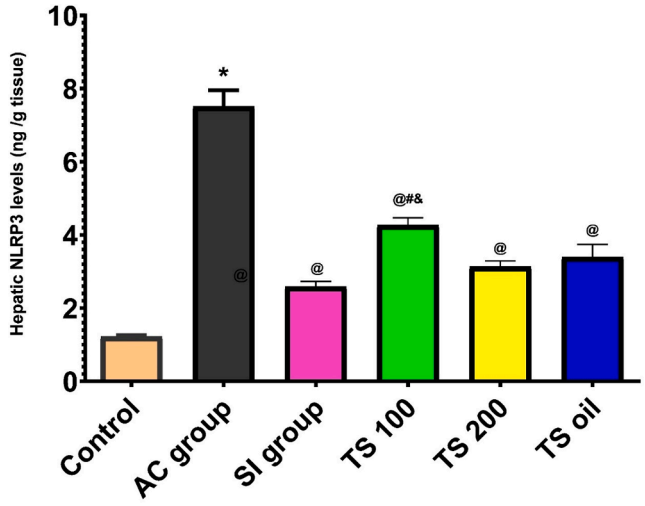

Fig. 8. Effect of acrylamide (AC, 25 mg/kg), *T. satureioides* extract (TS, 100 mg/kg and 200 mg/kg), *T. satureioides essential* oil (TS, 0.25 ml/kg) and silymarin (SI, 100 mg/kg) on hepatic levels of NLRP3 inflammasome in rats. Bars with error bars denote mean ± SE (n = 5). $^{*,@,\#,\&,\$}p < 0.05$ versus control group, acrylamide group, silymarin group, *T. satureioides* (200 mg/kg) extract group and essential oil group, respectively.

specimen in the different groups were assessed. This was done by using the Image J software as follow*:* H&E-stained hepatic slides of different groups were examined to calculate the area percentage of hepatocytes with hydropic degeneration which scattered in microscopic images captured at 400 ×. Scoring of each section was estimated according to the degree of degeneration as follows: 0 = no hydropic degeneration, 1 < 25 %, 2 = hydropic degeneration percent was between 25 % and 50 %, and 3 for > 50 % (Mohammed, 2020). MMP9 and TGF-β immunohistochemical stained sections of each studied group were examined to calculate the area percentage of positive immune cells which was done at the objective lens of 40x. The optical density for NF-κB and TNF-α immunohistochemical expression were measured at magnification × 400.

2.11. Statistical analysis

All data were expressed as the means ± standard error (SE) and analyzed using GraphPad Prism 8 statistic software (GraphPad Software, Inc., La Jolla, CA, USA). One-way analysis of variance (ANOVA) followed by post hoc Tukey's tests were adopted to evaluate the statistical comparisons between experimental groups. The Kruskal-Wallis's test was used to study the difference in histopathological scores. The $p < 0.05$ was considered statistically significant.

3. Results

3.1. Chemical profiling

GC–MS analysis of essential oil from *T. satureioides* furnished 39 compounds, Table 1 **and** Fig. 1**.** The major compounds were thymol (37.16%) followed by 2-methyl isoborneol (19.42%) and 2-octen-1-ol, anisole, *β*-caryophyllene, and *O*-cymene (12.89 %, 5.41 %, 3.73 %, and 3.14 %, respectively), while the other compounds were present at<3 %. Studies on *T. satureioides* EO highlighted borneol, thymol, carvacrol, camphene, pinene, terpineol, cymene, and linalool as major compounds. These were identified in our EO as well. LC-MS of analysis of the water extract from *T. satureioides* furnished 46 secondary metabolites belonging to phenolic acids, chalcones and flavonoids (Mahdi et al., 2023). As for phenolic acids, they included dihydroxybenzoic acid and its glucoside, chlorogenic acid, neochlorogenic acid, rosmarinic acid, salvianolic acid A and I, galloyl glucose, and caffeoyl glucose, among others (Mahdi et al., 2023). The chalcones contained resveratrol sulphate, and phloretic acid caffeate (Mahdi et al., Submitted). Several flavonoids were detected, among them *C*-glucosides such as apigenin di-*C*-glucoside, and *O*-glucosides, such as luteolin rutinoside, luteolin glucoside, luteolin glucuronide, quercetin glucuronide and quercetin rutinoside (Mahdi et al., 2023).

3.2. T. satureioides extract and its essential oil counteract acrylamide-induced liver injury in rats

As shown in Fig. 2, acrylamide-exposed rats displayed remarkable liver injury as manifested by dramatic increase in serum activities of liver enzymes AST, ALT and serum total bilirubin concentrations, as compared to control rats. Pretreatment of rats with *T. satureioides* extract at both dose levels (100 mg/kg and 200 mg/kg), significantly and similarly reduced serum activities of AST and ALT, as well as total bilirubin level, when compared to acrylamide-treated group. There were no significant differences among both dose levels of *T. satureioides* extract and silymarin-treated group regarding the studied parameters. On the other hand, *T. satureioides* essential oil significantly reduced

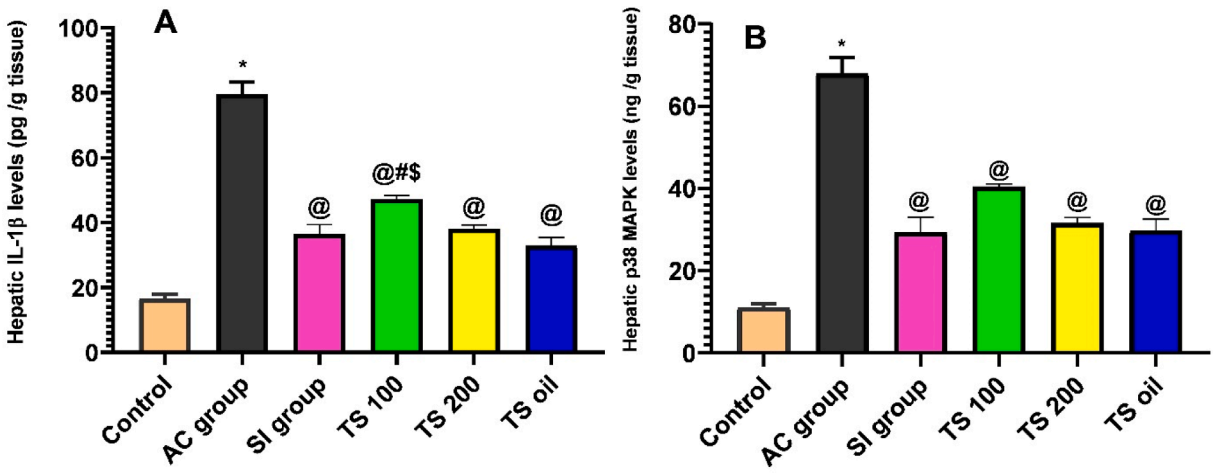

Fig. 9. Effect of acrylamide (AC, 25 mg/kg), *T. satureioides* extract (TS, 100 mg/kg and 200 mg/kg), *T. satureioides* essential oil (TS, 0.25 ml/kg) and silymarin (SI, 100 mg/kg) on hepatic levels of IL-1β (**A**) and p38 MAPK (**B**) in rats. Bars with error bars denote mean ± SE (n = 5). $^{*,@,\#,\&,\$}p < 0.05$ versus control group, acrylamide group, silymarin group, *T. satureioides* (200 mg/kg) extract group and essential oil group, respectively.

serum total bilirubin level and serum activity of ALT and tended to attenuate serum AST but did not reach statistical significance, when compared to acrylamide-treated group. Meanwhile, the effect of *T. satureioides* essential oil on serum AST activity is lower than that of silymarin ($p < 0.05$).

3.3. *T. satureioides extract and its essential oil reversed acrylamide-induced hepatic histological changes in rats*

Examination of liver specimens of control rats furnished well organized normal hepatic architecture. The portal area of control group appeared with thin-walled portal vein, bile duct with cuboidal lining and acidophilic hepatocytes with vesicular nucleus radiating around narrow sinusoids (Fig. 3**a**). Additionally, acidophilic hepatocytes were seen arranged as radiating cords around thin-walled central vein with thin sinusoids intervening between them (Fig. 3**aA**). Hepatic sections of acrylamide group showed disturbed liver architecture, some hepatocytes appeared with vacuolated cytoplasm and dark pyknotic nuclei. The portal area showed thick dilated portal vein, multiple dilated bile ducts and surrounded with inflammatory cell infiltrate (Fig. 3**bA**). Central vein appeared dilated with dilated liver sinusoids (Fig. 3**bB**). Liver specimens of both silymarin and *T. satureioides* (100 mg/kg) appeared with mild preservation of hepatic architecture, portal vein in both groups was moderately dilated, moderate inflammatory cell infiltrate appeared and few vacuolated hepatocytes with pyknotic nuclei (Fig. 3**c & dA**). Central vein and liver sinusoids were still dilated in hepatic sections of the same groups (Fig. 3**c & dB**). However, silymarin did not significantly affect hydropic cells scoring compared to acrylamide group ($p > 0.05$, Fig. 3**C**). Upon administration of *T. satureioides* (200 mg/kg) and *T. satureioides* essential oil, liver structure appeared markedly preserved with thin-walled portal vein, thin sinusoids, few pyknotic nuclei, few vacuolated cytoplasm and minimal inflammatory infiltrate (Fig. 3**e & fA**). The central vein of rats administrated the high dose of the extract was still thick walled and moderately dilated with minimal infiltrate (Fig. 3**eB**). Upon administration of the essential oil, a central vein appeared thin walled with thin sinusoids radiating from it (Fig. 3**fB**). Moreover, the extract at both dose levels and oil significantly decreased hydropic cells scoring compared to acrylamide group ($p < 0.05$, Fig. 3**C**).

3.4. *T. satureioides extract and essential oil ameliorated acrylamide-induced fibrotic changes liver tissue of rats*

3.4.1. *T. satureioides extract and essential oil attenuated acrylamide-induced collagen deposition*

To investigate whether *T. satureioides* extract and its essential oil can ameliorate fibrotic changes in liver, we stained liver tissues with Mallory trichrome that stained collagen fibers and measured MMP9 and TGF-1β immunoexpression. This study showed that the control group showed scanty collagen deposition around both portal and central veins (Fig. 4**a A&B**). Acrylamide induced marked deposition of collagen around dilated portal vein, bile ducts, hepatic artery, and central veins (Fig. 4**b A&B**). Meanwhile, both silymarin and *T. satureioides* (100 mg/kg) groups showed moderate deposition of collagen fiber around both portal and central veins (Fig. 4**c, d A&B**). There was minimal collagen deposition around portal and central vein areas upon administration of *T. satureioides* (200 mg/kg) and essential oil (Fig. 4**e.f A&B**).

3.4.2. *T. satureioides extract and its essential oil diminished acrylamide-induced fibrotic markers (MMP9 and TGF-1β) immunoexpression in liver tissue of rats*

We studied fibrotic markers (MMP9 and TGF-1β) in different groups to explain the observed changes in collagen deposition. This study showed that acrylamide increased immunoexpression of both fibrotic markers compared to the control group. All treatments reduced the two studied fibrotic markers compared to acrylamide. On the other hand, the high dose of the extract and the oil diminished the fibrotic markers more than silymarin. The essential oil seemed to produce the most potent antifibrotic effects (Figs. 5 & 6).

3.5. *T. satureioides extract and its essential oil ameliorated acrylamide-induced oxidative stress in liver tissue of rats*

Malondialdehyde (MDA) is the end-product of lipid peroxidation and assessed as a common oxidative stress marker. Administration of acrylamide to rats induced enhanced oxidative stress represented by a dramatic increase in MDA levels in their liver tissue, as compared to control group, Fig. 7**A**. Treatment of rats with both doses of *T. satureioides* extract or *T. satureioides* essential oil effectively normalized the MDA level in their liver tissue, as compared to acrylamide-treated group and to similar extent to that of silymarin-treated rats. GSH is the major intracellular antioxidant used to assess the antioxidant defense response. Acrylamide-treated group showed a significant decline in hepatic content of GSH, as compared to control group,

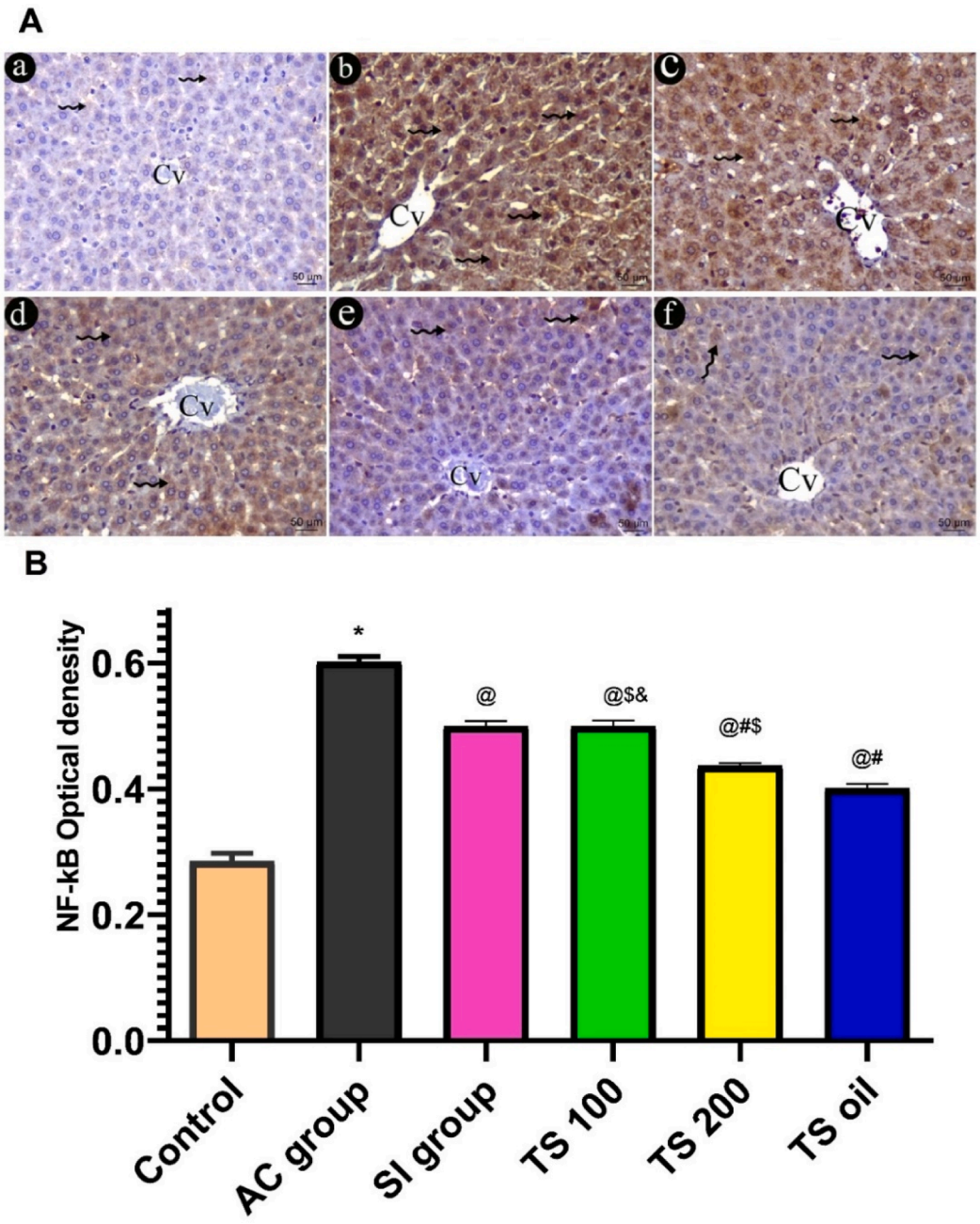

Fig. 10. Effect of acrylamide (AC, 25 mg/kg), *T. satureioides* extract (TS, 100 mg/kg and 200 mg/kg), *T. satureioides* essential oil (TS, 0.25 ml/kg) and silymarin (SI, 100 mg/kg) on hepatic levels of NF-κB in rats. Central vein (Cv), immune-positive cells (zigzag arrow), NF-κB immune-staining 400x. Bars with error bars denote mean ± SE (n = 5). $^{*,@,\#,\&,\$}p < 0.05$ versus control group, acrylamide group, silymarin group, *T. satureioides* (200 mg/kg) extract group and essential oil group, respectively.

indicating the exhaustion of the endogenous antioxidative defense system, Fig. 7**B**. Treatment of acrylamide-exposed rats with *T. satureioides* extract at both dose levels (100 mg/kg and 200 mg/kg), *T. satureioides* essential oil or silymarin significantly restored the hepatic content of GSH to that of control group, suggesting the antioxidant potential of *T. satureioides* extract. Notably, 100 mg/kg *T. satureioides* extract and silymarin induced much better effect on hepatic GSH levels than the higher dose of *T. satureioides* extract. The effect of 100 mg/kg *T. satureioides* extract and *T. satureioides* oil were comparable to that of silymarin regarding hepatic GSH, while 200 mg/kg *T. satureioides* extract was less than that of silymarin.

3.6. T. satureioides extract and its essential oil mitigated acrylamide induced NLRP3 upregulation in liver tissue of rats

NLRP3 plays a pivotal role in mediating inflammatory response and pyroptosis. As shown in Fig. 8, acrylamide exposure induced upregulation of hepatic levels of NLRP3 in rats, as compared to control group. *T. satureioides* extract and the oil exerted dose dependent reduction of the NLRP3 levels in liver tissue of rats, as compared to acrylamide-exposed rats, and to similar extent to that of silymarin therapy.

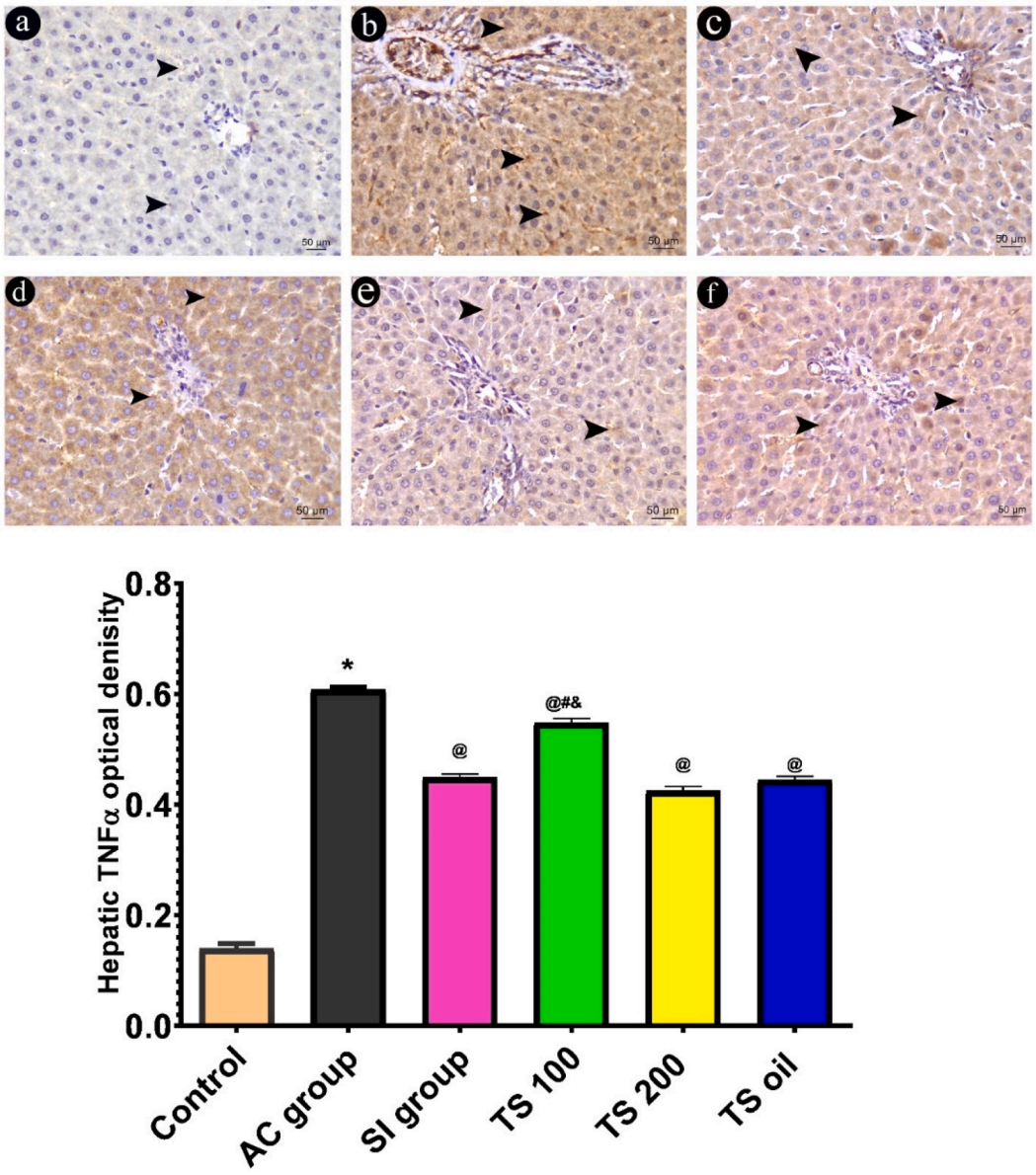

Fig. 11. Effect of acrylamide (AC, 25 mg/kg), *T. satureioides* extract (TS, 100 mg/kg and 200 mg/kg), *T. satureioides* essential oil (TS, 0.25 ml/kg) and silymarin (SI, 100 mg/kg) on hepatic levels of TNF-α in rats. Immune-positive cells (zigzag arrow), TNF-α immune-staining 400x. Bars with error bars denote mean ± SE (n = 5). $^{*,@,\#,\&,\$}p$ value < 0.05 versus control group, acrylamide group, silymarin group, *T. satureioides* (200 mg/kg) extract group and essential oil group, respectively.

3.7. T. satureioides extract and its essential oil alleviated acrylamide-induced inflammatory burden in liver tissue of rats

As shown in Fig. 9, there were significant increases in levels of IL-1β and p38 MAPK in hepatic tissue of rats subjected to acrylamide, as compared to control rats, implying to the augmented inflammatory response. Treatment of acrylamide-exposed rats with either both doses of *T. satureioides* extracts, *T. satureioides* essential oil or silymarin significantly attenuated the hepatic expression of IL-1β (Fig. 9**A**) and p38 MAPK (Fig. 9**B**), as compared to acrylamide-treated rats, suggesting the anti-inflammatory properties of *T. satureioides* extract. There were no significant differences among the anti-inflammatory effect of *T. satureioides* extract in a dose level 200 mg/kg, *T. satureioides* oil or silymarin regarding both parameters. Conversely, the suppressive effect of *T. satureioides* oil or silymarin on IL-1β levels was more superior to the lower dose of *T. satureioides* extract.

3.8. T. satureioides extract and its essential oil attenuated acrylamide-induced changes in NF-κB signaling in liver tissue of rats

We investigated NF-κB signaling by measuring immunoexpression of NF-κB and TNF-α in hepatic tissues of different studied groups (Figs. 10 & 11). We found that acrylamide augmented NF-κB immunoexpression and its downstream proinflammatory cytokine, TNF-α in hepatic tissues compared to normal control group. All treatments suppressed the expression of both markers compared to acrylamide group. The low dose of *T. satureioides* extract (100 mg/kg) exerted similar effects to silymarin, while the high dose of the extract and the essential oil exerted better effects on NF-κB than silymarin (Fig. 10). On the other hand, the essential oil induced the most potent inhibitory effect on hepatic TNF-α expression compared to silymarin and *T. satureioides* extract (Fig. 11).

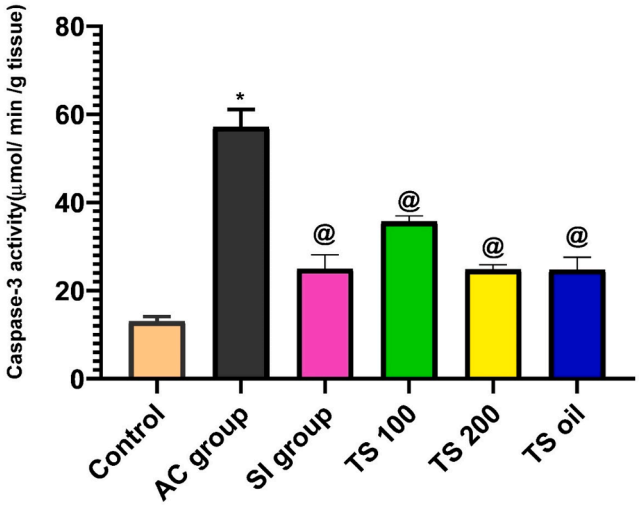

Fig. 12. Effect of acrylamide (AC, 25 mg/kg), *T. satureioides* extract (TS, 100 mg/kg and 200 mg/kg), *T. satureioides* oil (TS, 0.25 ml/kg) and silymarin (100 mg/kg) on caspase-3 activity in the liver tissue of rats. Bars with error bars denote mean ± SE (n = 5). $^{*,@}p < 0.05$, with respect to untreated control group and acrylamide-treated group, respectively.

3.9. T. satureioides extract and its essential oil offset acrylamide-induced apoptotic signaling in liver tissue of rats.

Caspase-3 exerts a crucial role in the execution-phase of cell apoptosis. As shown in Fig. 12, there was a significant increase in the caspase-3 activity in hepatic tissue of rats following exposure to acrylamide, as compared to control group, suggesting the activation of apoptotic signaling in liver cells, in consequence to acrylamide. Treatment of rats with either both doses of *T. satureioides* extracts, *T. satureioides* essential oil or silymarin significantly and similarly suppressed caspase-3 activity in their hepatic cells, as compared to acrylamide-treated rats, which might illustrate the anti-apoptotic potential of *T. satureioides* extract.

4. Discussion

This study aimed to investigate the hepatoprotective effects of *T. satureioides* polyphenolics and essential oil (EO) on acrylamide-induced hepatotoxicity. Acrylamide is a well-known food hydrophilic toxic substance that diffuse easily into the tissues upon uptake. One of the most affected organs by acrylamide exposure is liver as it has a central role in all metabolic processes (Abou-Seif et al., 2019). Here, we demonstrated that polyphenolics and EO from *T. satureioides* reversed the hepatic damage induced by acrylamide administration to rats. Acrylamide exposure weakened the capacity of the antioxidant defense system to neutralize ROS which disrupted the oxidation balance and increased lipid peroxidation leading to tissue damage (Makhlouf et al., 2011).

In this study, oral administration of acrylamide substantially increased serum liver enzymes AST, ALT, serum total bilirubin, and lipid peroxidation (MDA), decreased hepatic GSH, and altered liver architecture. However, pre-administration of the extract or EO significantly restored the liver enzymatic function. Increased GSH level is beneficial in neutralizing free radicals, stabilizing sulfhydryl groups and reducing hydrogen peroxide (Gedik et al., 2017). Moreover, free radicals induced by acrylamide deteriorated the structure of phospholipids in cell membranes. This broke down the cellular integrity which led to a significant augmentation in serum ALT and AST levels (Zamani et al., 2017). It also disrupted the ion gradients and membrane potential (Wong-ekkabut et al., 2007). Therefore, the increased serum levels of ALT and AST enzymes observed in this study could be explained by the release of these enzymes into the circulation system following the destruction of liver cell membrane integrity caused by acrylamide administration (Gedik et al., 2017). Similar findings were reported using other hepatotoxic agents such as carbon tetrachloride (El- Meligy et al., 2014)

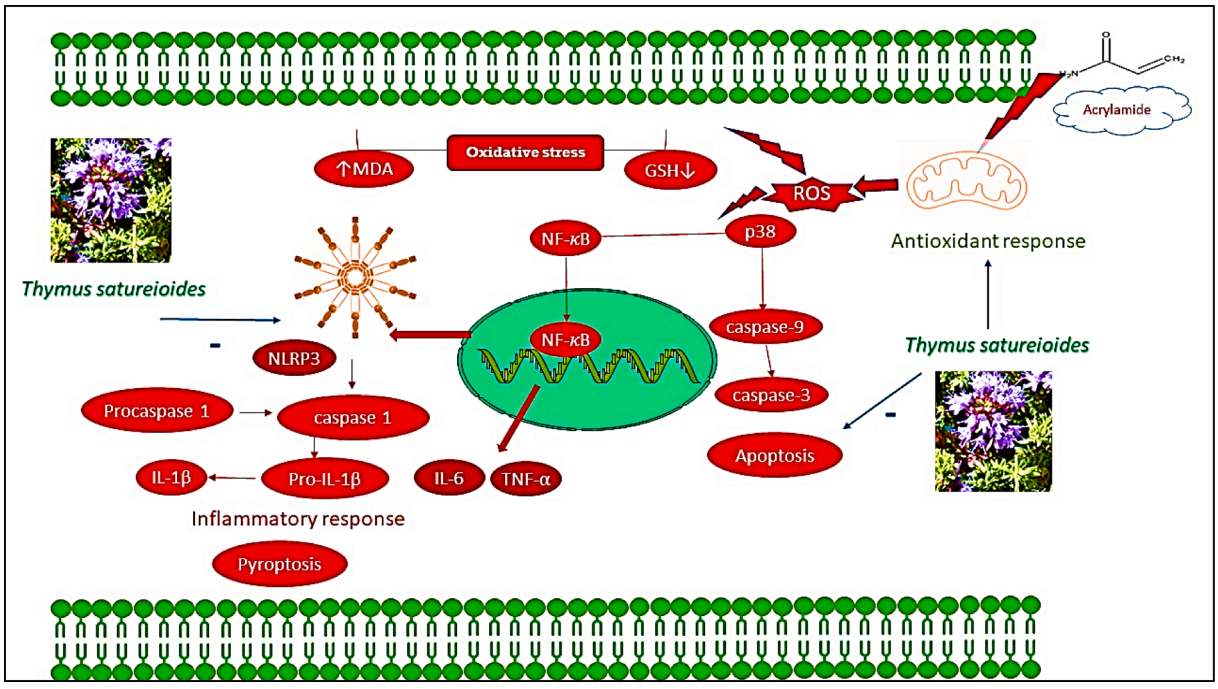

Fig. 13. Hepatoprotective activities of *T. satureioides* against acrylamide-induced hepatotoxicity. *T. satureioides* suppressed pyroptosis by inhibiting ROS generation and NLRP3 inflammasome expression in liver. This mitigated procaspase-1 cleavage to caspase-1 and generation of IL-β and thus inhibited pyroptosis. In addition, *T. satureioides* inhibited ROS-induced p38 MABP expression and consequently inhibited caspase-3 expression and apoptosis. It also suppressed P38 MAPK activation of NLRP3 inflammasome. Moreover, it inhibited NF-κB translocation and thus blocked the expression of various inflammatory cytokines including TNF-α and mitigated hepatic inflammation.

(Sobeh et al., 2018) and thioacetamide (Moustafa et al., 2014). Additionally, natural hepatoprotective compounds such as silymarin and silybin were reported to inhibit the penetration of toxic agents into the cells (AbouZid, 2012) and promote protein synthesis in hepatocytes (Sonnenbichler et al., 1986).

Here, we noticed that the biochemical parameters were correlated with histological alterations. Acrylamide induced congestion in central vein, sinusoids and vascular structures in the portal region, and inflammatory cell infiltration. These acrylamide-induced structural damages were also reported in previous studies (AbouZid, 2012; Karimi et al., 2020). However, pre-administration of the extract, EO, or silymarin preserved hepatic architecture, dilated portal vein, reduced inflammatory cell infiltration, and decreased vacuolated hepatocytes. Similar protective effects were reported using many plant-based molecules such as ellagic acid (Karimi et al., 2020), silymarin (AbouZid, 2012), and crocin (Gedik et al., 2017).

Another aspect of acrylamide liver toxicity is the accumulation of collagen fibers which is a precondition of hepatic fibrosis. Here, we revealed that acrylamide is indeed a profibrotic agent that induces remarkable collagen deposition around portal vein, bile ducts, hepatic artery, and central veins. Previous study has reported the same observations in the pituitary gland of acrylamide-treated male rats (NADHIM and AL-DERAWI, 2022). In this study, both silymarin and *T. satureioides* extracts and EO notably reduced this phenomenon as showed by minimal collagen deposition. As MMP9 and TGF-1β levels are biomarkers that predict collagen deposition (Ågren et al., 1998; Hughes et al., 2017), acrylamide administration also elevated their levels in liver tissues. Meanwhile, all treatments diminished the two studied fibrotic markers more than silymarin. MMP9 is also regarded a main indicator of the mitochondrial permeability that leads mitochondrial collapse and apoptosis (Chen et al., 2013). Hence, our extract and EO could also act on the mitochondria-dependent signaling pathways during exposure to oxidative stress. In addition, TGF-β1 is considered as a major driver of fibrosis in most tissues (Jiang et al., 2015) as it triggers the transition of cells into fibroblast-like cells that synthesize collagen. Moreover, it was reported that IL-1β could stimulate the production of TGF-β1 in rat hepatic stellate cell lines (Islam et al., 2014; Wang et al., 2016). Indeed, this study showed that the increases of IL-1β as well as p38 MAPK, a key regulator of pro-inflammatory cytokines biosynthesis, in hepatic tissue of rats subjected to acrylamide were mitigated using *T. satureioides* extract, EO or silymarin, suggesting their anti-inflammatory properties.

Inflammasomes are multi-protein complexes known to be induced under stress conditions. They are key mediators in acute and chronic inflammation *via* activation of pro-inflammatory cytokines (e.g., IL-1β and IL-18) (Garstkiewicz et al., 2017), and inflammatory caspases (e.g., caspase 1) (Jo et al., 2016). In fact, it is well documented that acrylamide induces NLRP3 inflammasome activation through ROS-MAPKs pathways (Bo et al., 2020). Moreover, ROS production could activate the MAPK signaling pathway which in turn activates NLRP3 and thus mediate inflammatory response and pyroptosis (Vanden Berghe et al., 1998). Activation of the NLRP3 inflammasome followed by IL-1β secretion amplifies inflammation and sensitivity of hepatocytes to liver injury (Petrasek et al., 2012). Hence, restraining the NLRP3 inflammasome is a potential strategy to prevent liver associated diseases (Sharma et al., 2022). Consistently, our findings demonstrated that acrylamide intoxication increases the levels of NLRP3 while the extract and EO treatments substantially alleviated its upregulation in liver tissues. Similar observations were reported following silibinin administration to mice with induced nonalcoholic fatty liver disease liver. This compound blocked caspase 1 cleavage and decreased NLRP3 inflammasome activation (Zhang et al., 2018). Likewise, mangiferin, a glucosylxanthone isolated from *Mangifera indica*, mitigated lipopolysaccharide and D-galactosamine-induced acute liver injury by potentiating the Nrf2 pathway and suppressing NLRP3 activation (Pan et al., 2016). Therefore, tested extracts and EO could potentially target the NLRP3 inflammasome and its downstream products, prevent obstructive symptoms, and reverse fibrotic changes induced by acrylamide toxicity.

As stated above, oxidative stress disturbs mitochondrial electron transfer chain complexes. This could lead to mitochondrial permeability transition and initiation of apoptosis via activation of caspase cascade (Zamani et al., 2017). We showed here that acrylamide exposure significantly increased caspase 3 activity, a crucial protein in the execution-phase of apoptosis, while *T. satureioides* polyphenols and EO suppressed caspase 3 activity in hepatic cells suggesting their anti-apoptotic potential. Other caspases such as caspase 9 and 8 were also shown to activate apoptosis pathway during immunotoxicity conditions induced by acrylamide (Kannan and Jain, 2000; Lee et al., 2014). These proapoptotic proteins were shown to be inhibited by many natural resources such as EO and compounds while to Bcl2, the anti-apoptotic protein, was increased (Hagar and Al Malki, 2014; Mahmoud et al., 2022; Zamani et al., 2017). Consequently, *T. satureioides* compounds potentially inhibited apoptosis signaling during acrylamide toxicity by preventing mitochondrial dysfunction (Fig. 13).

5. Conclusion

In this study, we demonstrated that *T. satureioides* polyphenolics and EO alleviated the acrylamide-induced liver injury by boosting antioxidant defense system, preventing hepatocytes damage, decreasing NF-κB and caspase 3 signaling pathways, and suppressing NLRP3 inflammasome activation in hepatocytes. The resulting reduction in IL-1β release substantially contributed to mitigating hepatic damage. These results suggest that inhibition of NLRP3 inflammasome/NF-κB axis by *T. satureioides* compounds is a promising strategy to prevent the pathological outcomes of acrylamide-induced liver injury. Nevertheless, further clinical trials are needed to confirm the role of natural inhibitors of NLRP3 inflammasome in preventing, treating, and managing xenobiotics-induced hepatotoxicity.

Ethical approval

The experimental design and animal handling procedures were revised and approved by the Ethical Committee for Animal Handling at Zagazig University (Approval No, ZU-IACUC/3/F/156/2022).

CRediT authorship contribution statement

Mansour So beh: Conceptulazation, Writing-review and editing.

Declaration of Competing Interest

The authors declare that they have no known competing financial interests or personal relationships that could have appeared to influence the work reported in this paper.

Data availability

No data was used for the research described in the article.

References

Abdel-Daim, M. M., Abo El-Ela, F. I., Alshahrani, F. K., Bin-Jumah, M., Al-Zharani, M., Almutairi, B., Alyousif, M. S., Bungau, S., Aleya, L., & Alkahtani, S. (2020). Protective effects of thymoquinone against acrylamide-induced liver, kidney and brain oxidative damage in rats. *Environmental Science and Pollution Research, 27*, 37709–37717. https://doi.org/10.1007/s11356-020-09516-3

Abou-Seif, H. S., Hozayen, W. G., & Hashem, K. S. (2019). Thymus vulgaris extract modulates dexamethasone induced liver injury and restores the hepatic antioxidant redox system. *Beni-Suef University Journal of Basic and Applied Sciences, 8*, 21. https://doi.org/10.1186/s43088-019-0021-0

AbouZid, S. (2012). *Silymarin, natural flavonolignans from milk thistle. Phytochemicals-A Global Perspective of Their Role in Nutrition and Health* (pp. 255–272). Rijeka: InTech.

Adams, A., Hamdani, S., Lancker, F. V., Méjri, S., & De Kimpe, N. (2010). Stability of acrylamide in model systems and its reactivity with selected nucleophiles. *Food*

Research International, 43, 1517–1522. https://doi.org/10.1016/j.foodres.2010.04.033

Ågren, M. S., Jorgensen, I. N., Andersen, M., Viljanto, J., & Gottrup, P. (1998). Matrix metalloproteinase 9 level predicts optimal collagen deposition during early wound repair in humans. *British Journal of Surgery, 85*, 68–71. https://doi.org/10.1046/j.1365-2168.1998.00556.x

Amrouche, T., Djenane, D., Dziri, F., Danoun, K., Djerbal, M., & Rabinal, P. R. (2018). Growth inhibition of Staphylococcus aureus, Bacillus cereus, and Escherichia coli assessed in vitro and in food system using thyme and mentha essential oils. *Systemes Agraires et Environnement, 2*, 01–10.

Asdadi, A., Alilou, H., Akssira, M., Mina, L., Hassani, I., & Chebli, B. (2014). Chemical composition and anticandidal effect of three thymus species essential oils from southwest of Morocco against the emerging nosocomial fluconazole-resistant strains. *Journal of Biology, Agriculture and Healthcare, 4*, 16–26.

Avato, P., Laquale, S., Argentieri, M. P., Lamiri, A., Radicci, V., & D'Addabbo, T. (2017). Nematicidal activity of essential oils from aromatic plants of Morocco. *Journal of Pest Science, 90*, 711–722. https://doi.org/10.1007/s10340-016-0805-0

Akahoshi, T., Hashizume, M., Tanoue, K., Shimabukuro, R., Gotoh, N., Tomikawa, M., & Sugimachi, K. (2002). Role of the spleen in liver fibrosis in rats may be mediated by transforming growth factor β-1. *Journal of gastroenterology and hepatology, 17*, 59–65.

Bancroft, J. (2013). *Layton C. Theory & practice of histological techniques* (7th ed., pp. 172–214). Philadelphia: Churchill Livingstone of Elsevier.

Kim, S. H., Kim, K., Ahn, J. H., & Chang, H. K. (2011). Increased expression of tumor necrosis factor-alpha in the rat hippocampus after acute homocysteine administration. *Journal of epilepsy research, 1*, 6.

Mohammed, H. (2020). Beneficial Role of Nigella Sativa Extracted Oil on the Hepato-toxic Effect of Ceftriaxone in Adult Male Albino Rat (Histological and Immuno-histochemical Study). *Journal of Medical Histology, 4*, 66–78.

Ramos-Vara, J., Kiupel, M., Baszler, T., Bliven, L., Brodersen, B., Chelack, B., Czub, S., Del Piero, F., Dial, S., & Ehrhart, E. (2008). American association of veterinary laboratory diagnosticians subcommittee on standardization of immunohistochemistry suggested guidelines for immunohistochemical techniques in veterinary diagnostic laboratories. *Journal of Veterinary Diagnostic Investigation, 20*, 393–413.

Sobeh, M., Mahmoud, M. F., Petruk, G., Rezq, S., Ashour, M. L., Youssef, F. S., El-Shazly, A. M., Monti, D. M., Abdel-Naim, A. B., & Wink, M. (2018). Syzygium aqueum: A polyphenol-rich leaf extract exhibits antioxidant, hepatoprotective, pain-killing and anti-inflammatory activities in animal models. *Frontiers in pharmacology, 9*, 566.

Xu, L., Ding, L., Wang, L., Cao, Y., Zhu, H., Lu, J., Xa, Li, Song, T., Hu, Y., & Dai, J. (2017). Umbilical cord-derived mesenchymal stem cells on scaffolds facilitate collagen degradation via upregulation of MMP-9 in rat uterine scars. *Stem Cell Research & Therapy, 8*, 1–13.

Bellakhdar, J., Claisse, R., Fleurentin, J., & Younos, C. (1991). Repertory of standard herbal drugs in the Moroccan pharmacopoea. *Journal of Ethnopharmacology, 35*, 123–143. https://doi.org/10.1016/0378-8741(91)90064-K

Benabid, A., 2000. Flore et écosystèmes du Maroc: Evaluation et préservation de la biodiversité.

Bo, N., Yilin, H., Haiyang, Y., & Yuan, Y. (2020). Acrylamide induced the activation of NLRP3 inflammasome via ROS-MAPKs pathways in Kupffer cells. *Food and Agricultural Immunology, 31*, 45–62. https://doi.org/10.1080/09540105.2019.1696284

Chen, J.-H., Yang, C.-H., Wang, Y.-S., Lee, J.-G., Cheng, C.-H., & Chou, C.-C. (2013). Acrylamide-induced mitochondria collapse and apoptosis in human astrocytoma cells. *Food and Chemical Toxicology, 51*, 446–452. https://doi.org/10.1016/j.fct.2012.10.025

El Hachlafi, N., Chebat, A., & Fikri-Benbrahim, K. (2021). Ethnopharmacology, Phytochemistry, and Pharmacological Properties of *Thymus satureioides* Coss. *Evidence-Based Complementary and Alternative Medicine, 2021*, 6673838. https://doi.org/10.1155/2021/6673838

El Hattabi, L., Talbaoui, A., Amzazi, S., Bakri, Y., Harhar, H., Costa, J., & Tabyaoui, M. (2016). Chemical composition and antibacterial activity of three essential oils from south of Morocco (Thymus satureoides, Thymus vulgaris and Chamaelum nobilis). *Journal of Materials and Environmental Science, 7*, 3110–3117.

El- Meligy, R., Zain, M., & Aly, F. (2014). Protective role of Cynanchum acutum L. extracts on carbon tetrachloride-induced hepatotoxicity in rat. *International Journal of Chemical and Applied Biological Sciences, 1*, 8–13. https://doi.org/10.4103/2348-0734.124349

el-Fassi Fihri, A., 1998. La pharmacopée marocaine traditionnelle, Jamal Bellakhdar. Horizons Maghrébins-Le droit à la mémoire 35, 319–321.

Elhelaly, A. E., AlBasher, G., Alfarraj, S., Almeer, R., Bahbah, E. I., Fouda, M. M. A., Bungău, S. G., Aleya, L., & Abdel-Daim, M. M. (2019). Protective effects of hesperidin and diosmin against acrylamide-induced liver, kidney, and brain oxidative damage in rats. *Environmental Science and Pollution Research, 26*, 35151–35162. https://doi.org/10.1007/s11356-019-06660-3

Erdemli, M. E., Altinoz, E., Aksungur, Z., Turkoz, Y., Dogan, Z., & Gozukara Bag, H. (2017). Biochemical investigation of the toxic effects of acrylamide administration during pregnancy on the liver of mother and fetus and the protective role of vitamin E. *Null, 30*, 844–848. https://doi.org/10.1080/14767058.2016.1188381

Erdemli, M. E., Arif Aladag, M., Altinoz, E., Demirtas, S., Turkoz, Y., Yigitcan, B., & Bag, H. G. (2018). Acrylamide applied during pregnancy causes the neurotoxic effect by lowering BDNF levels in the fetal brain. *Neurotoxicology and Teratology, 67*, 37–43. https://doi.org/10.1016/j.ntt.2018.03.005

Falzon, C. C., & Balabanova, A. (2017). Phytotherapy: An introduction to herbal medicine. *Primary Care: Clinics in Office Practice, 44*, 217–227. https://doi.org/10.1016/j.pop.2017.02.001

Friedman, M. A., Dulak, L. H., & Stedham, M. A. (1995). A Lifetime Oncogenicity Study in Rats with Acrylamide. *Fundamental and Applied Toxicology, 27*, 95–105. https://doi.org/10.1006/faat.1995.1112

Fuhr, U., Boettcher, M. I., Kinzig-Schippers, M., Weyer, A., Jetter, A., Lazar, A., Taubert, D., Tomalik-Scharte, D., Pournara, P., Jakob, V., Harlfinger, S., Klaassen, T., Berkessel, A., Angerer, J., Sörgel, F., & Schömig, E. (2006). Toxicokinetics of Acrylamide in Humans after Ingestion of a Defined Dose in a Test Meal to Improve Risk Assessment for Acrylamide Carcinogenicity. *Cancer Epidemiology, Biomarkers & Prevention, 15*, 266–271. https://doi.org/10.1158/1055-9965.EPI-05-0647

Garstkiewicz, M., Strittmatter, G. E., Grossi, S., Sand, J., Fenini, G., Werner, S., French, L. E., & Beer, H.-D. (2017). Opposing effects of Nrf2 and Nrf2-activating compounds on the NLRP3 inflammasome independent of Nrf2-mediated gene expression. *European Journal of Immunology, 47*, 806–817. https://doi.org/10.1002/eji.201646665

Gedik, S., Erdemli, M. E., Gul, M., Yigitcan, B., Gozukara Bag, H., Aksungur, Z., & Altinoz, E. (2017). Hepatoprotective effects of crocin on biochemical and histopathological alterations following acrylamide-induced liver injury in Wistar rats. *Biomedicine & Pharmacotherapy, 95*, 764–770. https://doi.org/10.1016/j.biopha.2017.08.139

Hagar, H., & Al Malki, W. (2014). Betaine supplementation protects against renal injury induced by cadmium intoxication in rats: Role of oxidative stress and caspase-3. *Environmental Toxicology and Pharmacology, 37*, 803–811. https://doi.org/10.1016/j.etap.2014.02.013

Haidara, M., Bourdy, G., De Tommasi, N., Braca, A., Traore, K., Giani, S., & Sanogo, R. (2016). Medicinal Plants Used in Mali for the Treatment of Malaria and Liver Diseases, 1934578X1601100309 *Natural Product Communications, 11*. https://doi.org/10.1177/1934578X1601100309.

Hughes, F. M., Sexton, S. J., Jin, H., Govada, V., & Purves, J. T. (2017). Bladder fibrosis during outlet obstruction is triggered through the NLRP3 inflammasome and the production of IL-1β. *American Journal of Physiology-Renal Physiology, 313*, F603–F610. https://doi.org/10.1152/ajprenal.00128.2017

Hussein, R. M., Anwar, M. M., Farghaly, H. S., & Kandeil, M. A. (2020). Gallic acid and ferulic acid protect the liver from thioacetamide-induced fibrosis in rats via differential expression of miR-21, miR-30 and miR-200 and impact on TGF-β1/Smad3 signaling. *Chemico-Biological Interactions, 324*, Article 109098. https://doi.org/10.1016/j.cbi.2020.109098

Islam, S. S., Mokhtari, R. B., El Hout, Y., Azadi, M. A., Alauddin, M., Yeger, H., & Farhat, W. A. (2014). TGF-β1 induces EMT reprogramming of porcine bladder urothelial cells into collagen producing fibroblasts-like cells in a Smad2/Smad3-dependent manner. *Journal of Cell Communication and Signaling, 8*, 39–58. https://doi.org/10.1007/s12079-013-0216-4

Jaafari, A., Mouse, H. A., Rakib, E. M., M'barek, L. A., Tilaoui, M., Benbakhta, C., Boulli, A., Abbad, A., & Zyad, A. (2007). Chemical composition and antitumor activity of different wild varieties of Moroccan thyme. *Revista Brasileira de Farmacognosia, 17*, 477–491. https://doi.org/10.1590/S0102-695X2007000400002

Jiang, G., Lei, A., Chen, Y., Yu, Q., Xie, J., Yang, Y., Yuan, T., & Su, D. (2021). The protective effects of the Ganoderma atrum polysaccharide against acrylamide-induced inflammation and oxidative damage in rats. *Food & function, 12*, 397–407. https://doi.org/10.1039/D0FO01873B

Jiang, X., Chen, Y., Zhu, H., Wang, B., Qu, P., Chen, R., & Sun, X. (2015). Sodium Tanshinone IIA Sulfonate Ameliorates Bladder Fibrosis in a Rat Model of Partial Bladder Outlet Obstruction by Inhibiting the TGF-β/Smad Pathway Activation. *PLoS One1, 10*, e0129655.

Jo, E.-K., Kim, J. K., Shin, D.-M., & Sasakawa, C. (2016). Molecular mechanisms regulating NLRP3 inflammasome activation. *Cellular & Molecular Immunology, 13*, 148–159. https://doi.org/10.1038/cmi.2015.95

Kabbaoui, M., Chda, A., Mejrhit, N., Azdad, O., Farah, A., Aarab, L., Bencheikh, R., & Tazi, A. (2016). Antidiabetic effect of *Thymus satureioides* aqueous extract in streptozotocin-induced diabetic rats. *International Journal of Pharmacy and Pharmaceutical Sciences, 8*, 140–145.

Kannan, K., & Jain, S. K. (2000). Oxidative stress and apoptosis. *Pathophysiology, 7*, 153–163. https://doi.org/10.1016/S0928-4680(00)00053-5

Karimi, M. Y., Fatemi, I., Kalantari, H., Mombeini, M. A., Mehrzadi, S., & Goudarzi, M. (2020). Ellagic Acid Prevents Oxidative Stress, Inflammation, and Histopathological Alterations in Acrylamide-Induced Hepatotoxicity in Wistar Rats. *Journal of Dietary Supplements, 17*, 651–662. https://doi.org/10.1080/19390211.2019.1634175

Kehrer, J. P., & Klotz, L.-O. (2015). Free radicals and related reactive species as mediators of tissue injury and disease: Implications for Health. *Null, 45*, 765–798. https://doi.org/10.3109/10408444.2015.1074159

Khouya, T., Ramchoun, M., Hmidani, A., Amrani, S., Harnafi, H., Benlyas, M., Filali Zegzouti, Y., & Alem, C. (2015). Anti-inflammatory, anticoagulant and antioxidant effects of aqueous extracts from Moroccan thyme varieties. *Asian Pacific Journal of Tropical Biomedicine, 5*, 636–644. https://doi.org/10.1016/j.apjtb.2015.05.011

Lee, J.-G., Wang, Y.-S., & Chou, C.-C. (2014). Acrylamide-induced apoptosis in rat primary astrocytes and human astrocytoma cell lines. *Toxicology in Vitro, 28*, 562–570. https://doi.org/10.1016/j.tiv.2014.01.005

Mahdi, I., Bakrim, W. B., Bitchagno, G. T. M., Annaz, H., Mahmoud, M. F., & Sobeh, M. (2022). Unraveling the Phytochemistry, Traditional Uses, and Biological and Pharmacological Activities of Thymus algeriensis Boiss. & Reut. *Oxidative Medicine and Cellular Longevity, 2022*, 6487430. https://doi.org/10.1155/2022/6487430

Mahdi, I., Fahsi, N., Annaz, H., Drissi, B., Barakate, M., Mahmoud, M. F., & Sobeh, M. (2023). Thymus satureioides Coss.: Mineral Composition, Nutritional Value, Phytochemical Profiling, and Dermatological Properties. *Molecules, 28*(12), 4636.

Mahmoud, M. F., Ali, N., Mostafa, I., Hasan, R. A., & Sobeh, M. (2022). Coriander Oil Reverses Dexamethasone-Induced Insulin Resistance in Rats. *Antioxidants, 11*. https://doi.org/10.3390/antiox11030441

Makhlouf, H., Saksouk, M., Habib, J., & Chahine, R. (2011). Determination of antioxidant activity of saffron taken from the flower of Crocus sativus grown in Lebanon. *African Journal of Biotechnology, 10*, 8093–8100. https://doi.org/10.5897/AJB11.406

Moorman, W. J., Reutman, S. S., Shaw, P. B., Blade, L. M., Marlow, D., Vesper, H., Clark, J. C., & Schrader, S. M. (2012). Occupational Exposure to Acrylamide in Closed System Production Plants: Air Levels and Biomonitoring. *Null, 75*, 100–111. https://doi.org/10.1080/15287394.2011.615109

Moustafa, A. H. A., Ali, E. M. M., Moselhey, S. S., Tousson, E., & El-Said, K. S. (2014). Effect of coriander on thioacetamide-induced hepatotoxicity in rats. *Toxicology and Industrial Health, 30*, 621–629. https://doi.org/10.1177/0748233712462470

Nadhim, A. A., & Al-Derawi, K. H. (2022). Histological, biochemical and chromosomal aberrations of pituitary gland induced by acrylamide in male rats. *Iranian Journal of Ichthyology, 9*, 412–423.

Pan, C., Pan, Z., Hu, J., Chen, W., Zhou, G., Lin, W., Jin, L., & Xu, C. (2016). Mangiferin alleviates lipopolysaccharide and D-galactosamine-induced acute liver injury by activating the Nrf2 pathway and inhibiting NLRP3 inflammasome activation. *European Journal of Pharmacology, 770*, 85–91. https://doi.org/10.1016/j.ejphar.2015.12.006

Petrasek, J., Bala, S., Csak, T., Lippai, D., Kodys, K., Menashy, V., Barrieau, M., Min, S.-Y., Kurt-Jones, E. A., & Szabo, G. (2012). IL-1 receptor antagonist ameliorates inflammasome-dependent alcoholic steatohepatitis in mice. *The Journal of Clinical Investigation, 122*, 3476–3489. https://doi.org/10.1172/JCI60777

Posadzki, P., Watson, L. K., & Ernst, E. (2013). Adverse effects of herbal medicines: An overview of systematic reviews. *Clinical Medicine, 13*, 7. https://doi.org/10.7861/clinmedicine.13-1-7

Ramchoun, M., Harnafi, H., Alem, C., Büchele, B., Simmet, T., Rouis, M., Atmani, F., & Amrani, S. (2012). Hypolipidemic and antioxidant effect of polyphenol-rich extracts from Moroccan thyme varieties. *e-SPEN Journal, 7*, e119–e124. https://doi.org/10.1016/j.clnme.2012.02.005

Santana, O., Andrés, M. F., Sanz, J., Errahmani, N., Abdeslam, L., & González-Coloma, A. (2014). Valorization of Essential Oils from Moroccan Aromatic Plants, 1934578X1400900812 *Natural Product Communications, 9*. https://doi.org/10.1177/1934578X1400900812.

Schuppan, D., Ashfaq-Khan, M., Yang, A. T., & Kim, Y. O. (2018). Liver fibrosis: Direct antifibrotic agents and targeted therapies. *Matrix Biology, 68–69*, 435–451. https://doi.org/10.1016/j.matbio.2018.04.006

Seto, W.-K., & Mandell, M. S. (2021). Chronic liver disease: Global perspectives and future challenges to delivering quality health care. *PLoS One1, 16*, e0243607.

Sharma, B., Satija, G., Madan, A., Garg, M., Alam, M. M., Shaquiquzzaman, M., Khanna, S., Tiwari, P., Parvez, S., Iqubal, A., Haque, S. E., & Khan, M. A. (2022). Role of NLRP3 Inflammasome and Its Inhibitors as Emerging Therapeutic Drug Candidate for Alzheimer's Disease: A Review of Mechanism of Activation, Regulation, and Inhibition. *Inflammation*. https://doi.org/10.1007/s10753-022-01730-0

Soliman, M. M., Alotaibi, S. S., Sayed, S., Hassan, M. M., Althobaiti, F., Aldhahrani, A., Youssef, G. B., & El-Shehawi, A. M. (2021). The Protective Impact of Salsola imbricata Leaf Extract From Taif Against Acrylamide-Induced Hepatic Inflammation and Oxidative Damage: The Role of Antioxidants, Cytokines, and Apoptosis-Associated Genes. *Frontiers in Veterinary Science, 8*. https://doi.org/10.3389/fvets.2021.817183

Sonnenbichler, J., Goldbero, M., Hane, L., Madubunyi, I., Vogl, S., & Zetl, I. (1986). Stimulatory effect of Silibinin on the DNA synthesis in partially hepatectomized rat livers: Non-response in hepatoma and other malign cell lines. *Biochemical Pharmacology, 35*, 538–541. https://doi.org/10.1016/0006-2952(86)90233-9

Tareke, E., Rydberg, P., Karlsson, P., Eriksson, S., & Törnqvist, M. (2002). Analysis of Acrylamide, a Carcinogen Formed in Heated Foodstuffs. *Journal of Agricultural and Food Chemistry, 50*, 4998–5006. https://doi.org/10.1021/jf020302f

Turkington, C., & Mitchell, D. (2010). *The encyclopedia of poisons and antidotes*. Facts On File.

Vanden Berghe, W., Plaisance, S., Boone, E., De Bosscher, K., Schmitz, M. L., Fiers, W., & Haegeman, G. (1998). p38 and Extracellular Signal-regulated Kinase Mitogen-activated Protein Kinase Pathways Are Required for Nuclear Factor-κB p65 Transactivation Mediated by Tumor Necrosis Factor*. *Journal of Biological Chemistry, 273*, 3285–3290. https://doi.org/10.1074/jbc.273.6.3285

Wang, H., Liu, S., Wang, Y., Chang, B., & Wang, B. (2016). Nod-like receptor protein 3 inflammasome activation by Escherichia coli RNA induces transforming growth factor beta 1 secretion in hepatic stellate cells. *Bosnian Journal of Basic Medical Sciences, 16*, 126–131, 10.17305/bjbms.2016.699.

Wong-ekkabut, J., Xu, Z., Triampo, W., Tang, I.-M., Peter Tieleman, D., & Monticelli, L. (2007). Effect of Lipid Peroxidation on the Properties of Lipid Bilayers: A Molecular Dynamics Study. *Biophysical Journal, 93*, 4225–4236. https://doi.org/10.1529/biophysj.107.112565

Zamani, E., Shaki, F., AbedianKenari, S., & Shokrzadeh, M. (2017). Acrylamide induces immunotoxicity through reactive oxygen species production and caspase-dependent apoptosis in mice splenocytes via the mitochondria-dependent signaling pathways. *Biomedicine & Pharmacotherapy, 94*, 523–530. https://doi.org/10.1016/j.biopha.2017.07.033

Zhang, B., Xu, D., She, L., Wang, Z., Yang, N., Sun, R., Zhang, Y., Yan, C., Wei, Q., Aa, J., Liu, B., Wang, G., & Xie, Y. (2018). Silybin inhibits NLRP3 inflammasome assembly through the NAD+/SIRT2 pathway in mice with nonalcoholic fatty liver disease. *The FASEB Journal, 32*, 757–767. https://doi.org/10.1096/fj.201700602R

New Clinical Study: Omegia™ Transforms Skin Health

We are delighted to share with you Puredia's latest achievement: the publication of a robust clinical study on our **Omegia™ sea buckthorn berry ingredients**, featured in the **Journal of Functional Foods**.

Key Findings from the Omegia™ Study:

Significant skin rejuvenation driven by **enhanced collagen production**
Boosted **skin hydration and elasticity** for a more youthful appearance
Reduction in signs of aging, including **wrinkles, redness, and pore size**
Improvement in **catalase activity and TNF-alpha** reduction

Beyond these skin health milestones, Omegia™ has been proven to aid in **alleviating vaginal dryness, dry eyes, and supporting cardiovascular function**. These findings underscore the versatility of Omegia™ as a comprehensive health solutions.

Journal of Functional Foods 112 (2024) 105973

Contents lists available at ScienceDirect

Journal of Functional Foods

journal homepage: www.elsevier.com/locate/jff

The impact of oral sea-buckthorn oil on skin, blood markers, ocular, and vaginal health: A randomized control trial

Leong-Perng Chan, Tung-Wen Yen, Ya-Ping Tseng, Tina Yuen, Michael Yuen, Hywel Yuen, Chia-Hua Liang

ARTICLE INFO

ABSTRACT

Sea buckthorn have been used for centuries as food and traditional medicine in Asia and Europe. This study

Why Incorporate Omegia™ in Your Product Line?
Science-Backed: Leverage the published clinical study to substantiate the health claims of your products.

Innovative: Offer a cutting-edge ingredient that is ahead of market trends.
Trusted: Provide your customers with a trusted solution that is both effective and safe.

If you're ready to enhance your supplement offerings with Omegia™, reach out to us, and let's innovate together.

Omega 3 6 7 9: Clinically-Supported for **Beauty** & **Menopause**

Clean & Vegan
One Softgel a Day
Superior Quality
Ready for Market
Available in oil & powder form
Sustainably & Responsibly Made